BRITISH ANTARCTIC SURVEY

SCIENTIFIC REPORTS

No. 106

DIFFUSE REFLECTIONS OF RADIO WAVES FROM THE IONOSPHERIC *F*-LAYER (SPREAD-*F*) OVER ARGENTINE ISLANDS, ANTARCTICA

By

A. S. RODGER, M.Sc.

Atmospheric Sciences Division, British Antarctic Survey

CAMBRIDGE: PUBLISHED BY THE BRITISH ANTARCTIC SURVEY: 1982

NATURAL ENVIRONMENT RESEARCH COUNCIL

DIFFUSE REFLECTIONS OF RADIO WAVES FROM THE IONOSPHERIC *F*-LAYER (SPREAD-*F*) OVER ARGENTINE ISLANDS, ANTARCTICA

By

A. S. RODGER, M.Sc.

Atmospheric Sciences Division, British Antarctic Survey

(Manuscript received 13 April 1982)

ABSTRACT

Spread-*F* is the term which denotes the presence of diffuse radio reflections from the *F*-region of the ionosphere either superposed upon or replacing the specular reflection from the *F*-layer, normally displayed on ionograms. The theory and phenology of Spread-*F* are briefly reviewed separately for equatorial, middle and high magnetic latitudes, and a short description of the various techniques used to investigate Spread-*F* is included. The occurrence of Spread-*F* over Argentine Islands, Antarctica (lat. 65° S, long. 64° W) is analysed in detail. A new method for quantifying the variations in Spread-*F* observed on ionograms is described. This technique is used to determine the diurnal, seasonal and solar-cycle variations of the phenomenon using Argentine Islands data for a continuous two-year period from March 1973 and for selected months over one and a half solar cycles. A further development of this quantifying method is used to establish the relationship between variations in the occurrence of Spread-*F* and magnetic activity.

A comparison of Spread-*F* as observed by an ionosonde and by a co-sited experiment employing the Doppler principle is presented. The simultaneous occurrence of Spread-*F* at magnetically conjugate points is also examined, and shown to be highly likely.

These analyses demonstrate several new and important results for an observatory at middle magnetic latitudes. It is suggested that at least four types of irregularities in the *F*-layer are required to explain the phenology of Spread-*F* observed at Argentine Islands. The variations of electron temperature and plasma concentration are shown to have many similarities to the variations in the occurrence of Spread-*F*, suggesting that plasma instabilities may be an important mechanism for the production and maintenance of irregularities causing Spread-*F* at Argentine Islands.

CONTENTS

	PAGE
I. Introduction	3
1. Definition of Spread-*F*	3
2. Scope of this report	3
II. Review of some theories of Spread-*F*	5
III. A brief review of the techniques for observing Spread-*F*	5
1. Vertical incidence sounding by ionosonde	5
2. Oblique incidence sounding by ionosonde	6
3. Doppler technique	6
4. Incoherent scatter radar	6
5. Scintillation	6
6. Topside sounding of the ionosphere and measurements *in situ* by satellites	6
7. Discussion	6
IV. The global phenology and morphology of Spread-*F*	7
1. Equatorial latitudes (dip angle 0–25°)	8
2. Middle latitudes (dip angle 25–60°)	8
3. High latitudes (dip angle 60–90°)	8
4. Artificially induced Spread-*F*	9
V. The classification of Spread-*F* on ionograms	9
VI. The study of Spread-*F* at Argentine Islands	9
1. Argentine Islands ionosonde data	9
2. Seasonal variation	11
3. Diurnal variation	12
4. Solar cycle variation	13
5. Variation with magnetic activity	14
a. A method of quantifying variations in Spread-*F* occurrence with magnetic activity	14
b. Variations with geomagnetic activity at sunspot minimum	14
c. Variations with geomagnetic activity at sunspot maximum	14
d. Variations with geomagnetic activity between 1700 and 1900 LT	15
6. Dependence on ionospheric parameters	15
a. Maximum electron concentration	15
b. *hmF2* and *ymF2*	16
7. Observations using the Doppler technique	16
a. Experimental methods	16
b. Interpretation of results	16
VII. The study of Spread-*F* at magnetically conjugate points	17
1. Correlation between Spread-*F* occurrences at geomagnetically conjugate points	17
2. Geomagnetic control of Spread-*F*	18
3. Geographic location and Spread-*F*	18
VIII. Interpretation and conclusions	19
1. Physical interpretation of ionogram classification	19
2. The size and orientation of irregularities	19
3. The diurnal, seasonal and solar cycle variations of Spread-*F*	19
4. Spread-*F* occurrence and geomagnetic activity	19
5. Spread-*F* and other ionospheric parameters	20
6. The H.F. Doppler experiment	20
7. Conjugate Spread-*F* observations	20
8. Mechanisms of Spread-*F* production	20
a. Phenology of mechanisms	20
b. Height of irregularities	21
c. Changes in recombination rate	21
d. Variations in production rate	21
e. Transport of ionization	21
f. Electron temperature and plasma concentration	22
9. Final remarks	24
IX. References	24

I. INTRODUCTION

1. *Definition of Spread-F*

Historically, the term Spread-*F* was introduced to denote the presence of diffuse radio reflections from the *F*-region of the ionosphere either superposed on, or replacing, the normal specular ray reflections from the *F*-layer. On ionograms, Spread-*F* appears as a diffuse pattern superposed on the normal trace (Fig. 1). The term Spread-*F* now encompasses other ionospheric phenomena, such as the scintillation of satellite signals or extra-terrestrial radio sources.

Although it is over 40 years since Spread-*F* was first reported and discussed (Appleton, 1937; Booker and Wells, 1938), there is still much to be learned about the phenomenon. It is generally accepted that Spread-*F* is a result of irregularities in the electron concentration in the *F*-region. These irregularities will be aligned with the magnetic field as the conductivity of ions and electrons parallel to the field is high and very much greater than that perpendicular to the field at *F*-region heights (> 200 km). This property allows the earth to be divided into three regions for the purpose of discussing Spread-*F*: an equatorial region, where the geomagnetic field is nearly horizontal (dip angle in the range 0–25°), a high latitude region where the field is nearly perpendicular to the earth (dip angle between 60 and 90°) and a middle latitude zone (dip angle between 25 and 60°) where neither approximation is appropriate.

Most examples of Spread-*F* can be classified into one of the two basic types, frequency spread and range spread. Frequency Spread-*F* is the term applied to diffuse reflection from a height near the maximum electron concentration, *hmF2,* in the *F*-region. Diffuse reflections occurring at heights well away from *hmF2* are termed range Spread-*F*. Ionograms showing examples of each are illustrated in Figs. 1b and 1c respectively, together with an ionogram showing no Spread-*F* (Fig. 1a). Piggott and Rawer (1978) discuss fully the appearance of frequency and range Spread-*F* on ionograms.

2. *Scope of this report*

First, current knowledge of Spread-*F* is reviewed. Both theoretical and observational evidence from all latitudes are included, the differences between equatorial, middle and high latitudes being particularly emphasized. The techniques for the classification and analysis of Spread-*F* are discussed with particular reference to the method used in this study, which is a modification of a system developed by Penndorf (1962*a*).

The results of analysing Spread-*F* on ionograms produced at Argentine Islands, Antarctica (lat. 65° S, long. 64° W, L = 2.4) form the second part of this report. The analysis employed data secured over a continuous two-year period from March 1973 and during selected months over one and a half solar cycles. The diurnal, seasonal and solar cycle (11 year) variations in the occurrence of Spread-*F* are established. In addition, the variations in occurrence of the phenomenon with changes of magnetic activity are analysed. It is shown that there is a high probability of Spread-*F* occurring simultaneously at magnetically conjugate points. Evidence from another ionospheric experiment, which utilizes the Doppler principle, is used to show that Spread-*F* reflections may be localized in height. The relationship between the occurrence of Spread-*F* and other ionospheric parameters is also considered.

In the final part, the implications of the observations made during this extensive study of the occurrence of Spread-*F* at Argentine Islands are considered. A brief discussion is given of influences possibly controlling the occurrence of Spread-*F*.

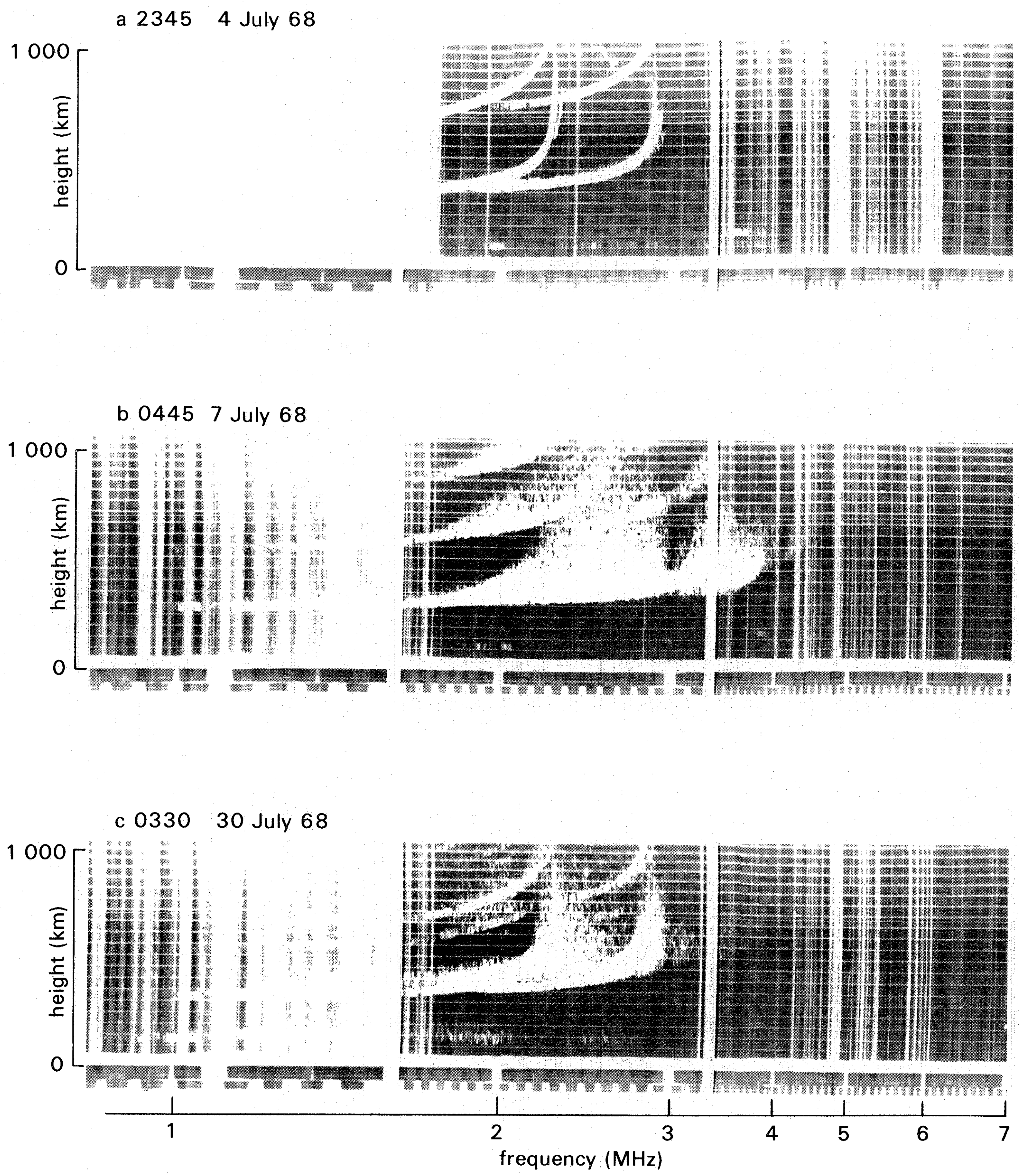

FIGURE 1
Argentine Islands ionograms showing:

a. No Spread-*F* echoes
b. Frequency Spread-*F* from 2.3 to 3.8 MHz as illustrated by the diffuse traces in the vicinity of the critical frequency
c. Range Spread-*F* from 1.2 to 2.2 MHz as illustrated by the diffuse echoes on the horizontal part of the echo trace. Frequency Spread-*F* is also present from 2.3 to 3.2 MHz.

II. REVIEW OF SOME THEORIES OF SPREAD-*F*

Although Spread-*F* has been identified from the earliest days of ionospheric research, the mechanisms responsible for the production at all latitudes of the field-aligned irregularities are not firmly established. In particular, there has been little theoretical work on mid-latitude Spread-*F*, though the global morphology of the phenomenon is now well established. One stumbling block in the development of Spread-*F* modelling has been that many workers believed the similar diffuse patterns observed on ionograms from all latitudes to be indicative of a single causative mechanism operating at all latitudes.

Early models, such as those by Renau (1959) and Farley (1963), suggested that the originating irregularity or scattering mechanism was in the *E*-region or in the valley between the *E*- and *F*-regions; the irregularity was then mapped into the *F*-region. Renau (1960) and Mawdsley and Ward (1960) were the first to propose that Spread-*F* is associated with field-aligned irregularities in the *F*-region. This was later confirmed experimentally by Farley (1967). The inconsistencies and limitations of these and other early models are reviewed by Farley and others (1970).

Spread-*F* in equatorial regions is now believed to be caused by the night-time westwards equatorial electrojet (Woodman, 1970). The electrojet flows at *E*-region heights but the Lorentz drift ($\boldsymbol{E} \wedge \boldsymbol{B}$), causes ionization to rise across the magnetic field lines in the early evening hours. If the upward velocity is large enough, plasma instabilities arise, and rapidly expand along the magnetic field lines. Currently, considerable research is being directed towards identifying the types of plasma instabilities involved (Kelley, 1979). A review of theories on equatorial Spread-*F* is given by Ossakow (1979).

At high latitudes, the variation in the occurrence of Spread-*F* with latitude is very similar to the distribution of charged particle precipitation. This was first noted by Herman (1966). Since then, this correlation has not been examined further. Some theoretical studies on high latitude irregularities have been carried out. These have mainly involved modifying equatorial region theory on irregularity formation for high latitudes. Fejer and Kelley (1980) have reviewed these studies. It should be noted that polar electrojets redistribute ionization horizontally and will not be important in the formation of *F*-region irregularities.

There has been very little work on mechanisms for the production of Spread-*F* at middle latitudes. Electrojets are not observed in this region except during severe magnetic disturbances, which are most unusual. Until recently it was believed that charged particle precipitation of magnetospheric origin was also unimportant, this phenomenon being mainly restricted to high latitudes (Rishbeth and Garriott, 1969). However, it has been suggested by many workers (e.g. Voss and Smith, 1980; Gledhill and Hoffman, 1981) that there may be a drizzle of low energy particles (< 20 keV) on all nights at geomagnetic mid-latitudes, which is not correlated with geomagnetic activity. The implications of this suggestion for Spread-*F* producing mechanisms have not yet been considered. Bowman (1960*a*, *b*, *c*) proposed that at least some types of Spread-*F*, such as range Spread-*F*, may be the result of wave-like structures in the isoionic contours of the *F*-region.

Some theoretical studies of the cause of geomagnetic mid-latitude Spread-*F* have been made by Perkins (1973) and further numerical simulation studies using the Perkins model were performed by Scannepieco and others (1975). However, both showed that some specific conditions on electron concentration gradients and electric fields were required and these have not been verified using ionospheric measurements.

Röttger (1976) suggested that Spread-*F* may result from an interaction between plasma drift and gravity waves. This may give rise to amplification, resonance and eventual breaking of the waves in a similar manner to water waves at a beach.

III. A BRIEF REVIEW OF THE TECHNIQUES FOR OBSERVING SPREAD-*F*

The characteristic dispersion or scattering of electromagnetic waves by the medium causing Spread-*F* can be detected over a wide band of frequencies, and with the transmitter and receiver either together or widely separated. In practice, the frequency range used to study Spread-*F* and its effects is 0.5–1000 MHz.

1. *Vertical incidence sounding by ionosonde*

An ionosonde measures the vertical distribution of electron concentration in the ionosphere by exploiting the fact that plasma of a certain concentration will reflect a radio wave of a given frequency (f) according to the relation

$$N_e \doteqdot 1.24 \times 10^{10} f^2,$$

where N_e is the electron concentration (m^{-3}) and f is in MHz. The time of flight of the signal gives the virtual height of reflection. Most ionosondes use a pulsed signal. The frequency is swept from about 1 to 20 MHz. Traditionally, signals are displayed on a two-dimensional calibrated plot of height against frequency, then recorded photographically (e.g. Fig. 1).

The earth's magnetic field causes an ionized medium to become doubly refracting. Thus, a radio wave incident on the bottom of the ionosphere is split into two components, an ordinary (o) and an extraordinary (x) wave, of opposite (circular or elliptical) polarizations. The electric vector of the o-wave becomes parallel to the magnetic field as the level of total refraction is approached, except under the condition when the wave is incident along the direction of the magnetic field. Thus the magnetic field has no effect on the condition of reflection. The x-wave is refracted so that its electric field is perpendicular to the magnetic field. Consequently, this reflection condition depends on the magnetic field strength in addition to the electron concentration. The maximum frequencies for the two waves (f_o and f_x) that can be reflected are related by the equation $f_x^2 - f_x f_b = f_o^2$ where f_b is the local value of the electron gyrofrequency. The horizontal separation of the points where total refraction of the o- and x-waves occurs (loosely termed reflection points) depends upon the dip angle and the distribution of underlying ionization, but typically for a mid-latitude *F*-region they may be between 15 and 20 km apart. (See Ratcliffe (1959) for a review of magneto-ionic theory.) A third mode of reflection (z) is possible. This occurs near the magnetic dip pole and can also be generated at low latitudes by scattering of energy from the *o*-wave in the direction of the magnetic field.

The ionosonde has the advantage of yielding information on the entire electron density distribution from the base of the *E*-region (height $\simeq$ 90 km) to the peak electron concentration of the *F2*-layer (*hmF2*) (height 200–500 km), but it only gives limited information from the valleys of ionization between the *E*- and *F*-regions.

2. *Oblique incidence sounding by ionosonde*

The technique of oblique incidence sounding by ionosonde differs from the conventional vertical incidence technique only in the respect that the transmitter and receiver are separated, usually by hundreds or thousands of kilometres. The advantage of the technique is that it can show the presence of the densest irregularities, even when they are a considerable distance from the mid-point of the path. However, there are severe difficulties in determining the location of the irregularities, as the propagation path of the signal is no longer along the great circle route. Also, at high latitudes, additional patterns dependent upon the geometry of the path are often generated by specular reflection from the field-aligned ionization structures produced by intense particle precipitation (Turunen and Oksman, 1979).

3. *Doppler technique*

A continuous fixed-frequency radio wave which has propagated via the ionosphere can show a Doppler shift if there is a change of phase path with time. When Spread-*F* is present, the received signal spectrum is considerably broader than that of signals unaffected by Spread-*F*. In the simplest technique employing this principle, the variation in the frequency received from a stable, fixed frequency transmitter such as WWV or WWVH is monitored. This type of experiment suffers from the same disadvantages as oblique incidence ionosondes.

4. *Incoherent scatter radar*

Incoherent scatter is the name given to the Thomson scatter of electromagnetic waves from individual electrons in the ionosphere. The returned signal amplitude yields information about electron concentration, and the Doppler broadening of reflected signals indicates electron temperature and ion mass. The precise shape of the reflected signal spectrum depends upon the ion to electron temperature ratio (allowing the ion temperature to be recovered) and the relative abundance of the principal ions present. Finally, the overall Doppler shift provides a measurement of the bulk motion of the plasma along the line of sight of the radar. A fuller description of the power and the limitations of the incoherent scatter experimental technique is given by Evans (1969, 1974), Farley and others (1970) and Petit (1975). This type of experiment shows the structure over the entire ionosphere up to about 800 km, including the interlayer valleys and the regions above *hmF2* which are not accessible with a conventional ionosonde. The experiment is very expensive both to build and operate. It requires very powerful transmitters, mostly operating between 50 MHz and 1 GHz, very sensitive receivers and complex aerial arrays. Consequently there are only a few such installations throughout the world.

Incoherent scatter radars have only been used extensively in equatorial regions to examine Spread-*F* in detail. Measurements of many features of Spread-*F*, such as the size and lifetime of irregularities, have been made (Farley, 1967; Kelley, 1979, and the references therein).

5. *Scintillation*

Scintillation of extra-terrestrial radio sources has been shown to be the result of irregularities in the ionosphere. Traditionally, astronomical radio sources were used as signal sources but more recently monitoring of artificial satellite transmissions has proved more practical (Titheridge, 1971; Frihagen, 1971). Most statistical studies of scintillation data use subjective measures of the depth of scintillations. Thus, comparison between scintillation results from various workers is not easy. Furthermore, it is impossible to determine at what height the irregularities are occurring, unless several stations are used.

6. *Topside sounding of the ionosphere and measurements in situ by satellites*

An orbiting satellite carrying an ionosonde can be used to give valuable information about the latitudinal and longitudinal extent of ionospheric structures above *hmF2*. This complements ground-based data for layers below *hmF2*. It can take several months to build up a complete set of observations to produce a diurnal variation pattern for one location, by which time seasonal variations may have influenced results. A satellite cannot distinguish between the separation of events in time, and a change with position. It is essential to link satellite data to ground-based data. Piggott and Rawer (1972) discuss the interpretation of these data and their matching to conventional ionograms.

Measurements *in situ* by satellite-borne experiments such as Langmuir probes (Brace and others, 1973) and retarding potential analyzers (Hanson and others, 1973) have provided high resolution observations of the variations in electron and ion concentration along the satellite path. With these data it has been possible to identify irregularities over a wide range of sizes from about 50 m to many kilometres.

7. *Discussion*

The information on irregularities provided by the different techniques described in the previous sections depends upon the shape and dimensions of the reflecting structure, the radio frequency used, the electron concentration and the gradient in electron concentration. The principal points may be collected under the headings of two physical conditions:

(i) *When the plasma frequency, f_n, is greater than the operating frequency, f_o.*

When $f_n > f_o$ and the reflecting structure is large compared with a Fresnel zone, a ray signal will be received, its amplitude varying with the apparent distance of the reflecting structure and the degree of absorption along its path. As the size of the structure decreases, the amplitude of the returned signal is correspondingly smaller. For a constant structure size, the amplitude of the returned signal increases with increasing frequency because the Fresnel zone decreases with increasing frequency.

(ii) *When the plasma frequency, f_n, is less than the operating frequency f_o.*

When $f_n < f_o$, the refractive index of the plasma, μ, for radio waves varies approximately as equation (1).

$$\mu^2 = 1 - (f_n/f_o)^2 \quad (1)$$

Assuming that $f_n^2/f_o^2 \ll 1$, then $\Delta\mu \simeq -f_n^2 - f_n^2/2f_o^2$, using a binomial expansion.

Partial reflections from steep gradients of refractive index are fairly common, and in this case the steepness of the gradient over the distance-scale of a wavelength in the medium is important. At sufficiently high frequencies, the boundary becomes slowly varying with wavelength and does not reflect. Thus, in general, low frequencies give reflections from structures larger than those that are seen at high frequencies.

The wavelength of an electromagnetic wave in the ionosphere (λ) is given by equation (2).

$$\lambda = c/\mu f \quad (2)$$

c is the speed of light in free space, f is the frequency of the wave and μ is the refractive index. Hence, as the refractive index decreases (electron concentration increases) the wavelength of the sounding wave increases and approaches infinity near the point of total refraction. This will be a significant factor in determining the size of irregularities that the various techniques will be able to detect.

On ionograms, 'satellite' traces will be seen when large irregularities (> 50 km) are present in the ionosphere. Superposition of satellite traces, which is most often seen away from critical frequencies, can be responsible for some range Spread-*F* traces (Bowman, 1960*a*, *b*; King, 1970). Smaller scale irregularities in the range of a few metres to a few hundred metres will, in general, cause diffuse traces to be seen on ionograms.

Scintillation measurements are usually made at relatively high frequencies. Therefore the discussions given in (ii) are important and scintillation data on Spread-*F* are heavily weighted by the presence of small-scale structures with large gradients in electron concentration.

The Doppler experiment measures the change of phase path, *P*, of a wave with time. The difference between the transmitted and received frequency, Δf, is related to *P* by equation (3) where λ is the wavelength:

$$\Delta f = -\frac{1}{\lambda}\frac{dP}{dt} \quad (3)$$

The phase path can be altered by vertical motion of the reflecting medium or by changes of refractive index along the path. When Spread-*F* is present, broadening of the received signal occurs. This can be interpreted as either irregularities moving randomly relative to each other (vertical motion) or could be caused by the continual formation and disappearance of irregularities (changes in refractive index). It is not possible to distinguish between these possibilities with the experimental technique.

As a rough guide to the sensitivities of the various techniques, an ionosonde can detect signals which have been attenuated by up to 30 dB compared with a signal reflected from a horizontally stratified, plane ionosphere. The power of partial reflection signals is approximately −70 dB and incoherent scatter a further 20 dB less. Booker (1956) suggested that Spread-*F* may be the result of partial reflections, but this type of signal is well below the threshold of an ionosonde. King (1970) has carried out a more detailed study of the power of partial and coherent reflections.

The differences in the data of the various techniques have been emphasized. However, to put them into perspective, some strong correlations between Spread-*F* observations by different experiments have been shown. For example, Koster and Wright (1960) showed a high correlation between scintillation data and Spread-*F* ionograms; Holtet and others (1976) have shown that electron density irregularities detected by incoherent scatter are well correlated with Spread-*F* on ionograms at the same locations. The relationship between Doppler broadening of signals and Spread-*F* is discussed in section VI.7. There is no substantive evidence that Spread-*F* on topside ionograms does not result from irregularities occurring below *hmF2*. King and others (1967) have found a few examples where topside data indicate irregularities, with none evident on ground-based data. This may be because the amplitude of the signals from the irregularities is below the threshold of the ground-based ionosonde, as there is additional attenuation of signals by the *D*, *E* and *F1*-layers in the bottomside ionosphere, these layers having no counterparts on the topside. Farley and others (1970) have shown that some irregularities may be restricted to above *hmF2* in equatorial regions, but this should be expected in a region where the magnetic field is nearly horizontal.

IV. THE GLOBAL PHENOLOGY AND MORPHOLOGY OF SPREAD-*F*

The percentage of all ionograms affected by Spread-*F*, irrespective of local time or date, is shown in Fig. 2 as a function of dip angle, for a year of moderate solar activity. The graph has been synthesized using the results of many surveys such as those by Singleton (1960, 1968), Shimazaki (1959, 1960), Penndorf (1962*b*, *c*), Frihagen (1971) and Chandra and Rastogi (1972). At any latitude, there are variations in the results which may range by about ± 10% from the values shown in Fig. 2. These arise principally from inconsistencies between the various sampling techniques used by different workers. Also, there are variations in the occurrence of Spread-*F* with longitude. Topside-sounder data (e.g. King and others, 1967) confirms the latitudinal distribution shown in Fig. 2.

Three different sampling methods are used in the studies of Spread-*F* occurrence using ionosondes. They are, in order of decreasing reliability, the scaling of Spread-*F* from ionograms, the use of *f*-plots, and the use of the *F*-notation

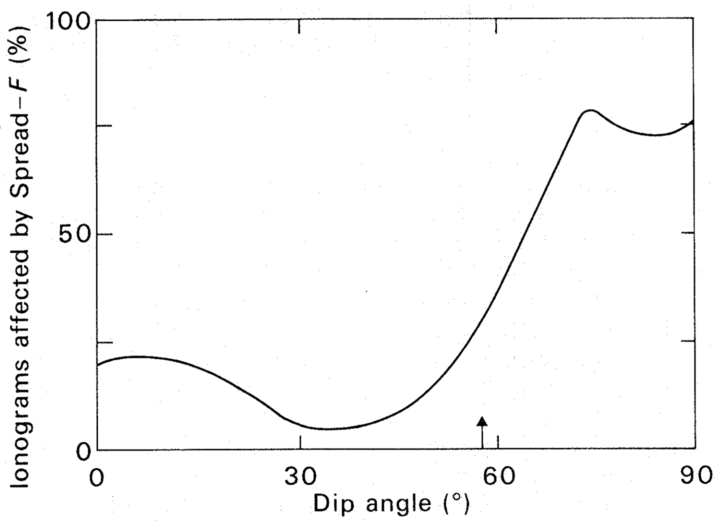

FIGURE 2

Percentage of ionograms showing Spread-*F* as a function of dip angle for a year of moderate solar activity. This figure is synthesized from a number of surveys of Spread-*F*, references being given in the text. The arrow indicates the dip angle of Argentine Islands.

(Piggott and Rawer, 1978) in published ionospheric data. The third method is by far the simplest and most widely adopted. However, it can be misleading, especially when range Spread-*F* is present, as this type of spreading does not necessarily obscure the standard parameters sufficiently to warrant the use of the *F*-notation. This principally affects results from equatorial regions where range Spread-*F* is the prevalent form.

1. *Equatorial latitudes (dip angle 0–25°)*

In equatorial regions Spread-*F* is extremely rare during daylight hours (Koster, 1958). Normally, range Spread-*F* first appears after sunset and is associated with a rapid rise in the height of the *F*-layer: both are caused by the $\boldsymbol{E} \wedge \boldsymbol{B}$ drift driven by the westward electrojet. Peak occurrence of range Spread-*F* is generally before midnight (Skinner and Kelleher, 1971). Frequency Spread-*F* is only about one-third as common as range Spread-*F* (Sastri and others, 1975) and is most likely to arise just prior to sunrise. King (1970) suggested that range Spread-*F* decays into frequency Spread-*F* during the night. Recent observational evidence (Kelley, 1979) suggests that irregularities with scale sizes of kilometres are generated first, but small-scale irregularities rapidly evolve from them. Theoretical simulations (Ossakow, 1979) also show this cascading effect from large to small irregularities. There is little seasonal variation in occurrence of Spread-*F* (Clemensha, 1964).

The solar cycle variation in the occurrence of equatorial Spread-*F* has been shown (Skinner and Kelleher, 1971) to have a longitudinal dependence. Over Africa and Asia, Spread-*F* is positively correlated with solar activity but the converse is true in the American zone. No satisfactory explanation has been proposed for this observation.

Shimazaki (1959, 1960) has shown that Spread-*F* is less likely to occur during periods of magnetic activity. This is consistent with the electrojet mechanism for Spread-*F* as the equatorial electrojet is less intense during periods of magnetic activity.

2. *Middle latitudes (dip angle 25–60°)*

In middle latitudes, the occurrence of Spread-*F* is infrequent compared with both high and equatorial latitudes. Little theoretical work has been carried out for this region, but the morphology and phenology is reasonably well established. Frequency Spread-*F* is the more common form of spreading and is most likely to occur between sunset and sunrise (Briggs, 1958; Singleton, 1957). Spread-*F* is comparatively rare during the day (Kasuya and others, 1955). Seasonal variations show minima at the equinoxes with a large winter solstice maximum and a less pronounced peak at the summer solstice (Shimazaki, 1959, 1960). Shimazaki also showed a strong inverse solar cycle relationship and a positive correlation between the occurrence of Spread-*F* and geomagnetic activity. More recent work by Bowman (1971, 1979) suggests that the maximum increase in Spread-*F* occurrence may arise several days after the time of maximum geomagnetic activity.

3. *High latitudes (dip angle 60–90°)*

The occurrence of Spread-*F* increases rapidly from about 60° dip angle towards the pole, with a maximum at or near the auroral oval (Penndorf, 1962*b*). Singleton (1969) found a significant minimum in Spread-*F* occurrence between the auroral oval maximum and the dip pole, using the *F*-notation in published data books. There is a strong maximum in the occurrence of Spread-*F* in winter and a deep minimum in summer. Spread-*F* mostly occurs between sunset and sunrise but is a more common phenomenon in daytime at high latitudes than at equatorial and middle latitudes.

Penndorf (1962*b*) has reported that there is an area in northern Canada where Spread-*F* occurrence varies neither diurnally nor seasonally. This area moves with the solar cycle, drifting towards the magnetic pole with increasing solar activity. No equivalent zone has been found in the southern hemisphere but the density of ionospheric observatories there is considerably less.

The variations in the occurrence of Spread-*F* resulting from increased geomagnetic activity are difficult to establish at high latitudes using ionosondes, because of the high incidence of blackout during such periods. Blackout is said to occur when ionospheric absorption is sufficiently large that no echoes are observed on an ionogram (Rodger and others, 1981). It happens frequently during periods of high geomagnetic activity and also while the sun is not illuminating the ionosphere; both of these factors may seriously affect Spread-*F* data.

Scintillation data from high latitudes confirm the approximate latitude profile given in Fig. 2, but Frihagen (1970) found that the minimum reported by Singleton (1969) was less significant and about 5° closer to the dip pole, i.e. near 80°. He also showed that the depth of scintillations and the level of geomagnetic activity were directly correlated. However, Spread-*F* on ionograms and scintillations are not necessarily caused by the same irregularities. Frihagen (1970) has compared observations by these two techniques at high latitudes and shown good consistency between them.

Aarons and others (1969) have reported that there is often a sharp boundary to the high latitude scintillations and Bates (1971) notices the same effect on ionospheric backscatter data.

4. *Artificially induced Spread-F*

Spread-*F* has been induced artificially under two circumstances, namely by a high altitude nuclear explosion (Heisler and Wilson, 1962) and by ionospheric heating experiments (Utlaut, 1970; Allen and others, 1974). It is not within the scope of this work to discuss this type of Spread-*F*, but it is interesting to note that when frequency Spread-*F* was created by the heating experiment the Spread-*F* appeared on the low frequency side of the main trace. This is most unusual under normal conditions.

V. THE CLASSIFICATION OF SPREAD-*F* ON IONOGRAMS

A distinction has been drawn between two basic types of Spread-*F* pattern appearing on ionograms: range spread and frequency spread, but a more detailed classification scheme is required in order to extend the study of the morphology of Spread-*F*. Several schemes have been proposed such as those suggested by Renau (1960), Rao and others (1960), Penndorf (1962*a*), INAG (1969) and Piggott and Rawer (1972). The Penndorf method was considered to be most suitable for Spread-*F* analysis at Argentine Islands because it gives the most detailed description, but is also simple to use.

In Penndorf's system, a Spread-*F* pattern on an ionogram may be allocated to one of five groups, depending upon its visual appearance. The five classes are labelled by the Greek letters α, β, γ, δ and ϵ. Each group is further subdivided according to the degree of spreading, on a scale from one to five, the highest numbers indicating the most Spread-*F*. This number is represented by the symbol *Ip* and termed the 'weighting factor'.

Although this scheme was originally developed for use in the northern auroral zone, about 97% of all Spread-*F* patterns observed at Argentine Islands could be adequately described by using one or more of Penndorf's types. Two new types (ζ and η) were defined to describe the remaining 3%. Line drawings of all the types observed at Argentine Islands are shown in Fig. 3.

This scheme is based upon pattern classification only and there is no physical basis *a priori* for the division between the various types. There are also some practical difficulties in its use. For example, the extent of Spread-*F* varies slightly between classes for the same weighting factor. It can be easily seen in Fig. 3 that $\beta2$ shows more spreading than $\alpha2$. Consequently, comparison of the occurrence of the various classes of Spread-*F* should be interpreted qualitatively rather than quantitatively.

In some of the more severely spread classes, e.g. $\alpha3$, $\beta3$ and $\gamma5$, Penndorf (1962*a*) assumes that some degree of range spread is present. However, this range spread is not always observed on Argentine Islands ionograms. In all cases where ionograms displayed severe spreading, any range Spread-*F* (δ-class) present was recorded as a separate observation in addition to the frequency Spread-*F*. The Spread-*F* pattern on the original ionogram may thus be regarded as a superposition of two patterns of different classes. Consequently consistency of interpretation of Spread-*F* patterns is obtained.

The scheme does not take into account cases when the Spread-*F* on the *o*- and *x*-traces are different either in pattern or the degree of spreading. In the case of pattern difference, the *o*-mode is always scaled for Argentine Islands and in the case of degree of spreading, the trace showing the greater spreading is used. In most examples this is the *o*-trace because the non-deviative absorption for the *x*-mode is always greater than for the *o*-mode. Also magneto-ionic effects tend to bend the *o*-mode ray so that it is perpendicular to the field line; hence any field-aligned irregularity will have a larger effective cross-sectional area to an *o*-mode wave than to the *x*-mode.

Polar spur traces (Piggott and Rawer, 1978) are not included in Penndorf's scheme, although they are a relatively common Spread-*F* pattern at some stations. This is acceptable for analysis of the Spread-*F* as polar spur traces are reflections from obliquity and not representative of conditions over the observatory. Finally, Penndorf's scheme is independent of the value of *foF2* which is tabulated separately when relations between Spread-*F* and *foF2* are required. This is discussed in section VI.6.

VI. THE STUDY OF SPREAD-*F* AT ARGENTINE ISLANDS

The advantages of the Antarctic and especially the Weddell Sea–Antarctic Peninsula zone for ionospheric research have been discussed by Piggott (1977) and by Dudeney and Piggott (1978). The main advantage is the relative displacement of the geographic, dip and invariant coordinate systems which is large when compared with the northern hemisphere. Consequently, effects caused by solar illumination (ionization), dynamic processes (thermospheric winds, electric fields) and magnetospheric phenomena (polar wind, particle precipitation), should be more easily resolved in the South than in the North.

1. *Argentine Islands ionosonde data*

The use of ionospheric data from Argentine Islands (geophysical parameters are given in Table I) has some special advantages. There is a nearly complete set of data of a very high standard spanning over 20 years. A geomagnetic observatory has been in operation since 1963, and between 1976 and 1979 an H.F. Doppler experiment was installed; these provide very useful complementary data.

The conjugate magnetic point to Argentine Islands, as evaluated by Barrish and Roederer (1969) using the internal field expansion model, is 37° N, 67° W. The ionospheric observa-

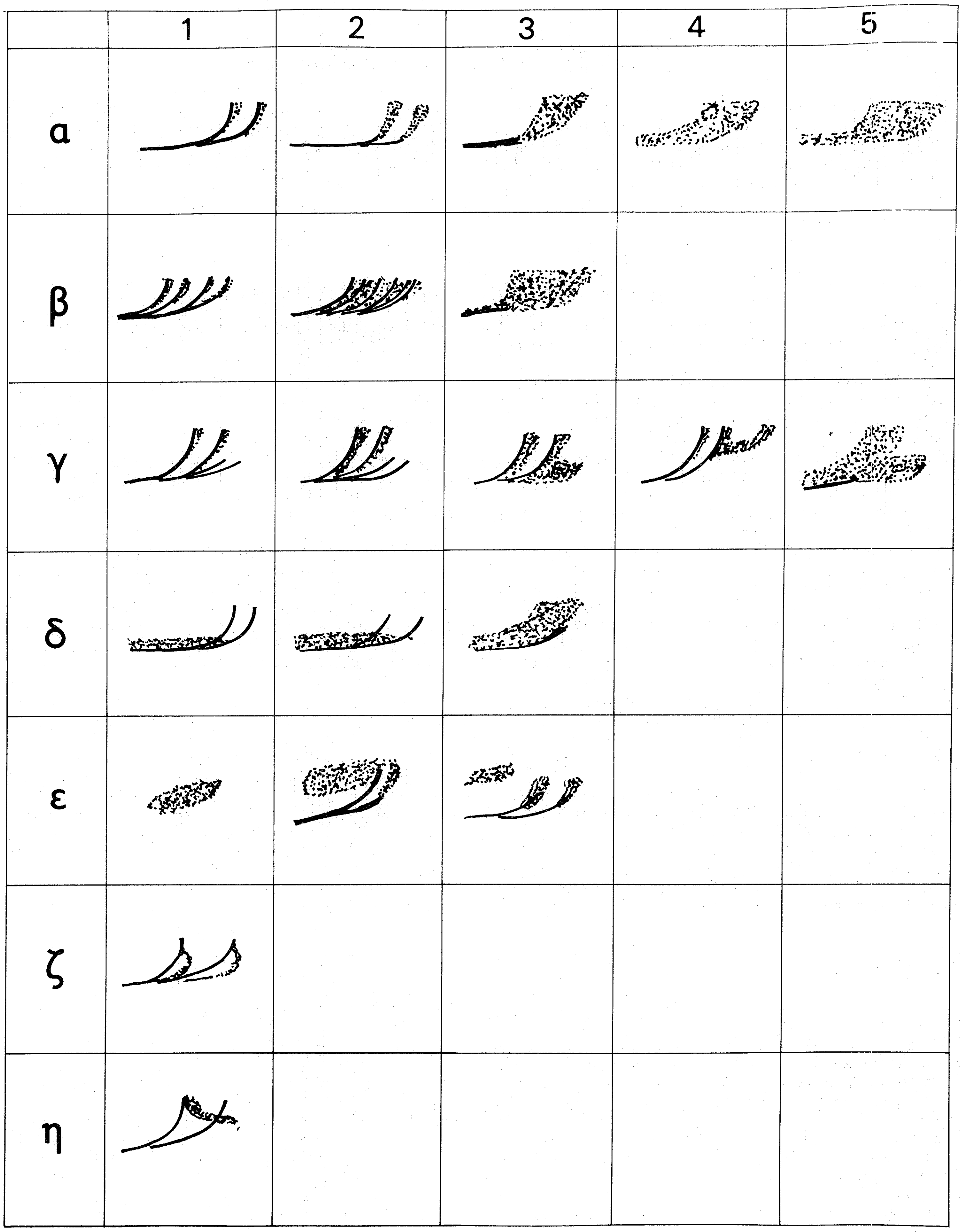

FIGURE 3
The patterns of Spread-*F* echoes as classified by Penndorf (1962*a*). Also included are two new classes, ζ and η, which were required to describe about 3% of Spread-*F* patterns observed at Argentine Islands.

TABLE I

GEOPHYSICAL AND GEOMAGNETIC DATA FOR ARGENTINE ISLANDS

Geographic coordinates	65.2° S, 64.3° W
Geomagnetic coordinates	− 53.7°, − 3.3°
Dip angle	− 57.9°
Dip latitude	− 38.6°
L-shell value	2.4
Invariant latitude	− 49.6°
Time meridian	60° W (local time, LT = UT − 4 h)

Note: Invariant latitude = arcsec $\sqrt{L}$. See McIlwain (1961) for a full explanation of this coordinate system.

tory at Wallops Island (lat. 38° N, long. 75° W) is not exactly conjugate, but close enough to study conjugate ionospheric effects. This pair of stations have the principal advantage of being separated by only 40 min in local time. This is most important in the study of those conjugate effects which may be solar controlled.

Argentine Islands (see Table I), where the dip angle is − 57.9°, lies close to the boundary between high and mid-latitudes which may be taken to be 60° for work on Spread-*F*. Consequently, the observatory is ideally situated to observe a significant amount of mid-latitude-type Spread-*F* but will also see a proportion of high latitude Spread-*F* patterns. Also, blackout is comparatively rare at Argentine Islands, so there is little (about 0.02%) data loss.

The modified Penndorf scheme was used to classify the Spread-*F* patterns on all the hourly ionograms for a 2-year period commencing March 1973. In addition, the ionograms for the month of July in the years 1957–59 and 1962–74 were classified to determine solar cycle variations.

TABLE II

DETAILS OF IONOSONDE EQUIPMENT AND PROGRAMME OF SOUNDINGS AT ARGENTINE ISLANDS

Ionosonde type	Union Radio Mark II Serial No. 22		
Frequency range	Band 1	0.6 to 1.4 MHz	0–1 min after start
	Band 2	1.4 to 3.2 MHz	1–2 min after start
	Band 3	3.2 to 7.0 MHz	2–3 min after start
	*Band 4	7.0 to 15.0 MHz	3–4 min after start
	*Band 5	15.0 to 25.0 MHz	4–5 min after start
Accuracy of timing	Passes through 3 MHz on the hour ± 15 s		
Peak power	Approximately 1 kW		
Pulse repetition frequency	50 pps		
Pulse length	Normally 240 μs but can be varied from 80 to 330 μs		
Aerial	Terminated vertical rhombics		
Sounding programme	1957–68 hourly, and subsequently every 15 min		

* Use optional.

A summary of the technical details of the Union Radio Mark II ionosonde used at Argentine Islands is given in Table II. A full description of the equipment is given by Clarke and Shearman (1953). Tests were carried out to ensure the reliability and consistency of the Spread-*F* data. These show the presence of few, relatively small anomalies. The most important are those in July 1967 when the summed values of *Ip* were unexpectedly high and in July 1969 when they were low. This is explained by the abnormally high and low receiver gain settings adopted at the station in these years. The reliability of the data between March 1973 and February 1975 is exceptionally good, although equipment problems caused slightly less Spread-*F* to be observed for May, June and July 1973 than would have been expected. The ionosonde site and the aerial array were relocated in 1961 from Port Lockroy (lat. 64.8° S, long. 63.5° W) to Argentine Islands (lat. 65.2° S, long. 64.3° W), a distance of 48 km, but, as expected, there is no detectable discontinuity in the Spread-*F* data at this time.

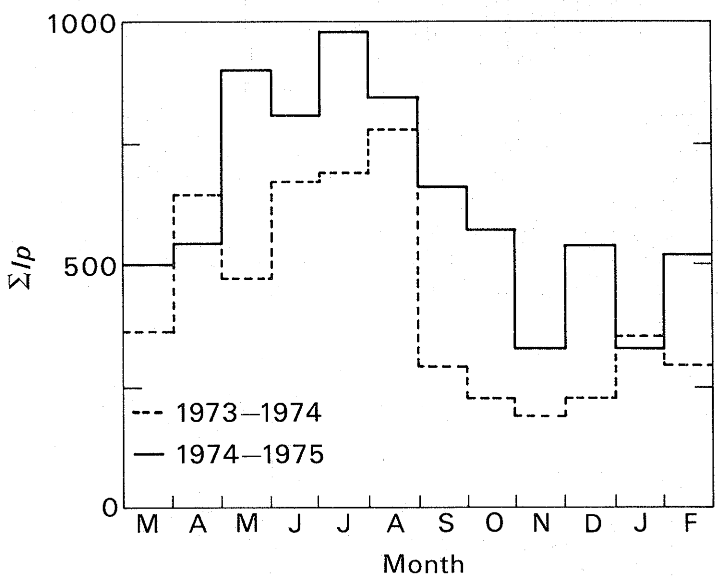

FIGURE 4

The monthly variation in the occurrence of Spread-*F* at Argentine Islands from March 1973 to February 1975, a sunspot minimum epoch.

2. *Seasonal variation*

The weighting factors (*Ip*) from the hourly observation of Spread-*F* were added together to produce monthly totals of *Ip* for every month in the period March 1973 to February 1975. The results are shown in Fig. 4. No adjustments have been made to take account of the small differences in the lengths of months. There is a strong seasonal variation, with a maximum at the winter solstice and a minimum near the summer solstice. The mean monthly total of *Ip* over the whole year from March 1973 was 430. This increased to 630 for the year from

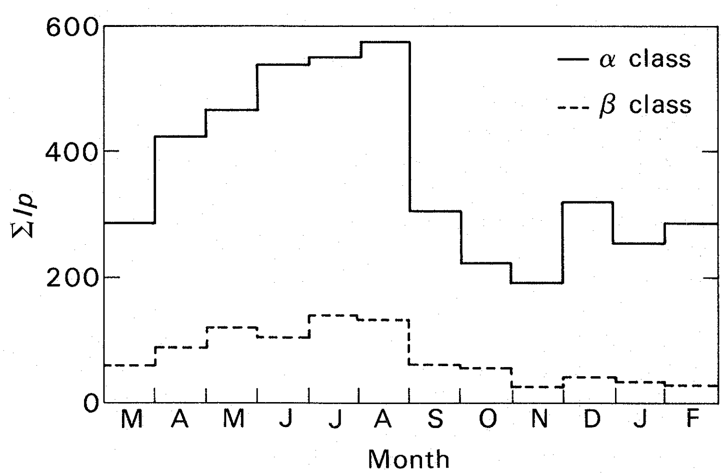

FIGURE 5

The monthly variation in the occurrence of α and β class Spread-*F* at Argentine Islands. Data for the years 1973–74 and 1974–75 have been averaged.

March 1974. April 1973 was magnetically very active and caused the amount of Spread-*F* observed at Argentine Islands to increase.

Only three Penndorf classes of Spread-*F* patterns (α, β and δ) were sufficiently common for their seasonal occurrence to be studied individually. Both α and β classes (Fig. 5) show a seasonal distribution very similar to that of total Spread-*F* (Fig. 4). This is hardly surprising since these classes constitute about 70 and 15% of the total respectively. The seasonal pattern of the δ class differs significantly from both α and β. There are two maxima, on the summer side of the equinoxes, the October peak being larger than that in February. This is clearly shown in Fig. 6 where the monthly totals of *Ip* for δ class are shown as a percentage of the ΣIp in that month. Geomagnetic activity was on average slightly higher in the months of October compared with the months of February; this may explain the difference in the magnitudes of the peaks.

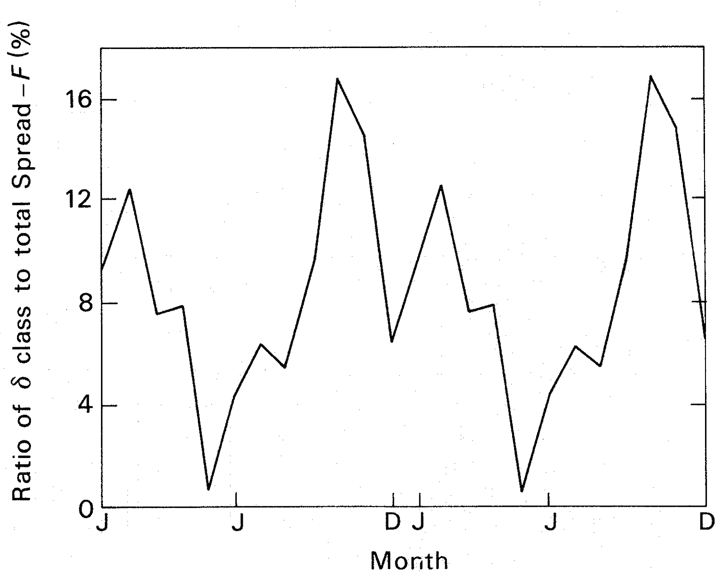

FIGURE 6
The monthly variation of the summed *Ip* for δ class Spread-*F* as a percentage of the total Spread-*F* (ΣIp) observed. The data for the years 1973–74 and 1974–75 have been averaged, but two complete cycles are shown.

3. *The diurnal variation*

In order to determine the diurnal variation of Spread-*F*, hourly totals of *Ip* were made. The data for the four summer months (November, December, January and February) and four winter months (May, June, July and August) have been separately averaged and are shown in Fig. 7. During the summer months, the sun does not set on the *F*-region. As shown in the seasonal variation patterns, there is appreciably more Spread-*F* observed in winter than in summer during every hour. The maximum occurrence of Spread-*F* comes after midnight, the summer and winter peaks occurring near 0100 and 0300 LT respectively. This 2 h time shift is not regarded as significant. In winter much more Spread-*F* is observed between 1600 and 2200 LT than would be expected from the summer pattern. If Spread-*F* occurs after local sunset, it usually persists for the rest of the night until local sunrise.

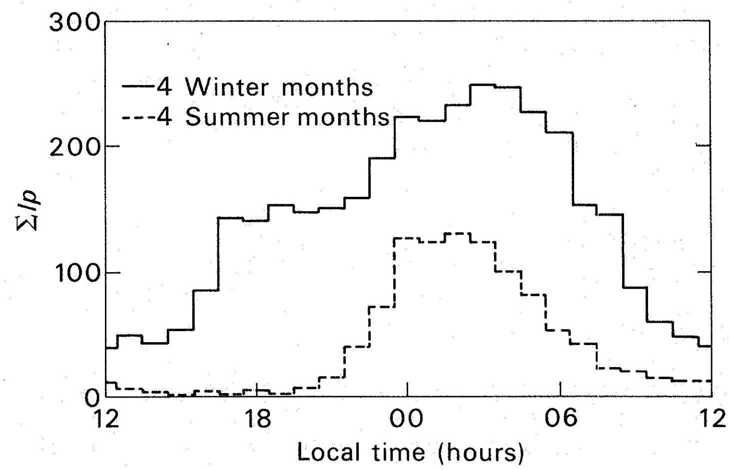

FIGURE 7
The mean diurnal variation in the occurrence of Spread-*F* at Argentine Islands at sunspot minimum.

The diurnal variations in the occurrence of α and β classes of Spread-*F* (Figs. 8 and 9 respectively) again show strong resemblances to that of total Spread-*F* with maxima at 0300 and 0400 LT. However, δ class shows a very sharp peak centred on local midnight (Fig. 10), some 3–4 h earlier than α and β classes. The winter sub-maximum at 1600–2200 LT is not associated with δ class Spread-*F*.

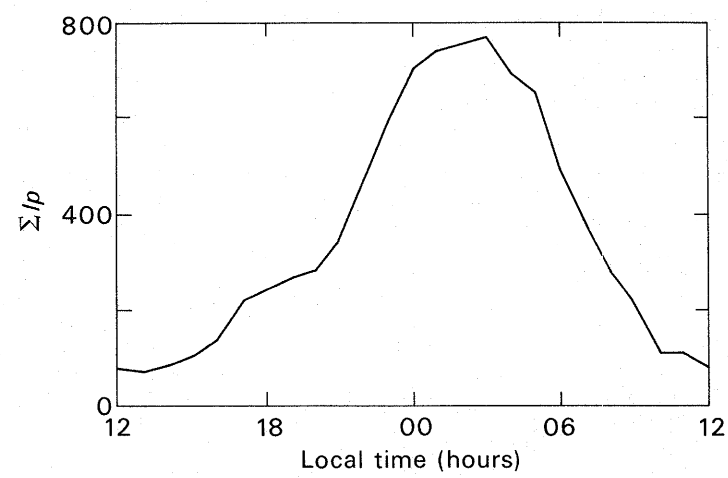

FIGURE 8
The diurnal variation in the occurrence of α class Spread-*F* for the period March 1973 to February 1975.

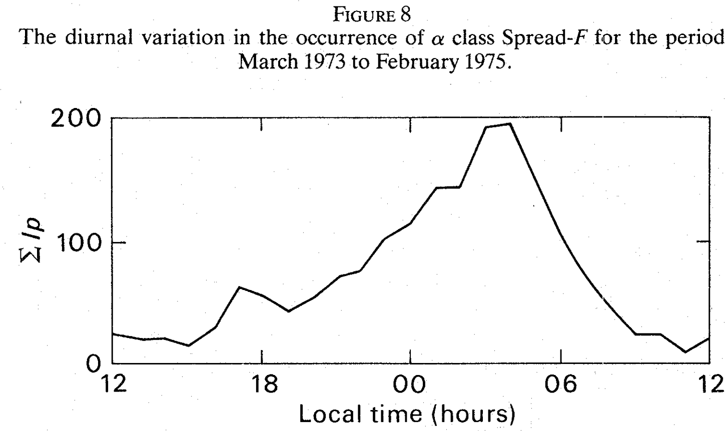

FIGURE 9
The diurnal variation in the occurrence of β class Spread-*F* for the period March 1973 to February 1975.

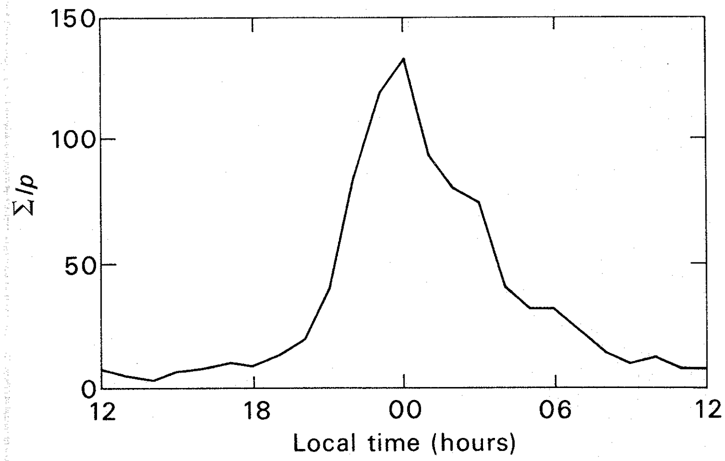

FIGURE 10
The diurnal variation in the occurrence of δ class Spread-*F* for the period March 1973 to February 1975.

4. *Solar cycle variation*
July was selected as the representative month for each year as sufficient Spread-*F* occurs during the austral winter months at all epochs of the solar cycle to provide a statistically significant sample. *Ip* totals were evaluated for every July between 1957 and 1974 with the exception of 1960 and 1961 when the data quality was poor. Sunspot maximum is defined here as those months when the mean daily value of solar flux at a wavelength of 10.7 cm was greater than 135×10^{-22} W m^{-2} Hz^{-1}, namely 1957–59 and 1967–70. Sunspot minimum is taken to be when the daily mean flux for the Julys fell below 95×10^{-22} W m^{-2} Hz^{-1}. This includes the years 1962–65, 1973 and 1974.

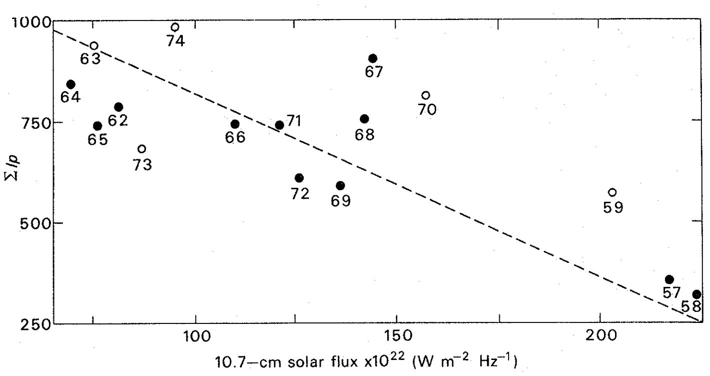

FIGURE 11
The summed *Ip* totals for the months of July in various years between 1957 and 1974, plotted against the mean 10.7-cm solar flux for that month. Points are labelled with the year. ● magnetically quiet months ($\Sigma Ap < 500$); ○ magnetically active months ($\Sigma Ap > 500$). – – – line of best fit through the magnetically quiet months.

The *Ip* for each sample month is plotted (Fig. 11) against the mean daily value of 10.7-cm solar flux for that month as a measure of solar activity. The data have been divided into two groups: the magnetically quiet months in which the summed daily values of the geomagnetic index, $\Sigma Ap < 500$ (represented by filled circles), and the active months in which $\Sigma Ap > 500$ (shown as open circles). The figure reveals that the occurrence of Spread-*F* at Argentine Islands is inversely correlated with solar activity. The line of best fit has been drawn for the magnetically quiet months shown in the figure. All months of high activity ($\Sigma Ap > 500$) lie above this line with the exception of 1973 when the measurements were anomalously low because of equipment problems.

The mean diurnal variation in the occurrence of Spread-*F* in the months of July at both sunspot maximum and minimum is shown in Fig. 12. These diurnal variations are very similar, with the maximum occurrence being shortly after midnight; a sub-maximum at about 1800 LT and a minimum near local noon appear for both epochs. More Spread-*F* is observed during sunspot minimum than during sunspot maximum at almost all times.

Fig. 13, shows the ratio of the ΣIp at solar minimum to that at solar maximum from Fig. 12. It is clear that the greatest variations occur near 1100 LT, with a subsidiary peak near local midnight. There are also three periods when the amount

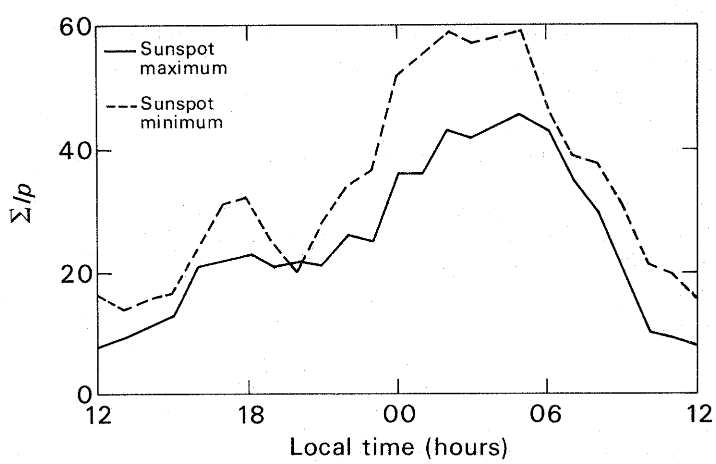

FIGURE 12
The mean diurnal variation in Spread-*F* in the months of July at sunspot maximum (mean of data from 6 years) and at sunspot minimum (mean of data from 8 years). (Maximum and minimum defined in the text.)

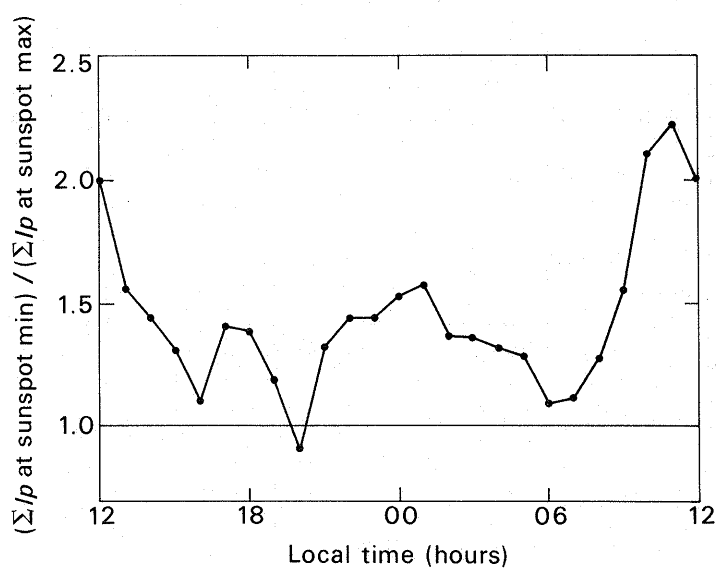

FIGURE 13
The diurnal variation of the ratio (ΣIp at sunspot minimum)/(ΣIp at sunspot maximum).

TABLE III

THE RELATIVE OCCURRENCE OF α, β AND δ CLASSES OF SPREAD-*F* AT SUNSPOT MAXIMUM AND MINIMUM

	Sunspot maximum		*Sunspot minimum*	
Class of spread	*Percentage of total spread*	*Standard deviation*	*Percentage of total spread*	*Standard deviation*
α	68.1	± 5.7	73.8	± 6.9
β	18.1	± 5.9	15.2	± 3.1
δ	5.5	± 3.2	3.2	± 2.5

Note: The standard deviations have been evaluated using the Bessel correction factor.

of Spread-*F* observed is approximately the same at both sunspot maximum and minimum, namely 1600, 1900–2000 and 0600–0700 LT.

Table III shows that the relative occurrence of α, β and δ classes of Spread-*F* for July does not change through the solar cycle, to within experimental uncertainty.

5. *The variations in the occurrence of Spread-F with magnetic activity*

a. *A method for quantifying variations in Spread-F occurrence with magnetic activity.* Variations in the occurrence of Spread-*F* with magnetic activity can be quantified using the formula given by equation (4).

$$Ik = \frac{1}{N}\left[\sum_{0}^{N} Ip\, n(Ip)\right] \tag{4}$$

It gives an indication of Spread-*F* per hour, *Ik,* as a function of geomagnetic activity. *n(Ip)* is the number of Spread-*F* weighting factors at each of the levels, $Ip = 0$–5. *N* is the total number of observations for each level of magnetic activity, $K = 0$–9. *K* is the international magnetic index and is approximately logarithmic in magnetic perturbation amplitude.

The *K* magnetic index used for all data after 1973 was that determined at the local observatory at Argentine Islands. Prior to this date the planetary magnetic index, *Kp,* was used as this was more readily available. A detailed comparison of these two indices shows no significant difference for the purposes of this study and data determined using these indices may be directly compared.

b. *Variation with geomagnetic activity at sunspot minimum.* The relationship between the occurrence of Spread-*F*, *Ik*, and geomagnetic activity, *K*, at Argentine Islands, was established for sunspot minimum epoch on the basis of data taken between March 1973 and February 1975. The data for the summer and winter months are shown in Fig. 14. The relatively small number of cases with $K > 6$ have been amalgamated with those at $K = 6$ and plotted at $K = 6$. Geomagnetic activity and Spread-*F* occurrence are positively correlated at both solstices. The correlation coefficients for the best-fit straight lines are 0.98 and 0.97 for winter and summer respectively, and the gradients of the lines are the same, within experimental uncertainty. The lines were determined giving all points equal weighting. The intercept of the

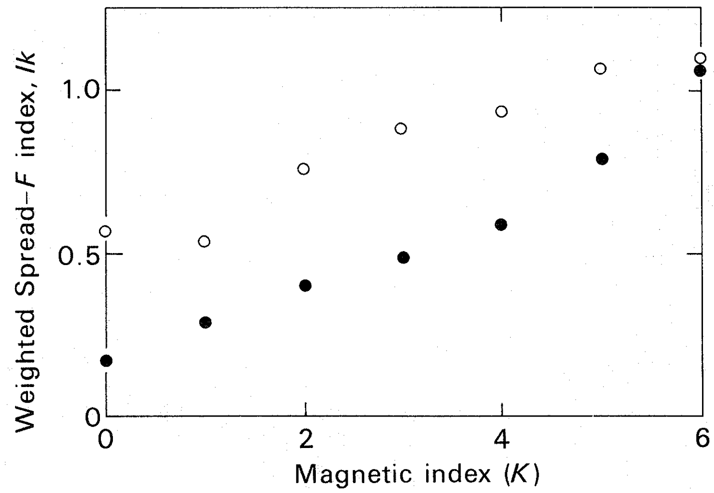

FIGURE 14

The variation in the occurrence of Spread-*F* at Argentine Islands with geomagnetic activity at sunspot minimum. The *K* magnetic index is determined from the observatory's recordings. All data for $K \geq 6$ have been amalgamated and plotted at $K = 6$. ○ winter months (May–August); ● summer months (November–February).

winter lines on the abscissa is considerably greater than that of the summer line as expected from the seasonal analysis (Fig. 4).

c. *Variations with geomagnetic activity at sunspot maximum.* An investigation similar to that described above was carried out for a sunspot maximum period using data for the months of July 1957–59 and 1967–69. The results are illustrated in Fig. 15. All data for $Kp \geq 8$ have been amalgamated and plotted at $Kp = 8$. There is a slight negative correlation between Spread-*F* occurrence and geomagnetic activity up to $Kp = 5$. For these points, the Spread-*F* observed has been dominated by low values of weighting factor. The correlation coefficient of the best-fit straight line, determined giving all points equal weight, is 0.88. For $Kp > 5$, there is a significant jump in the intensity of Spread-*F*. These

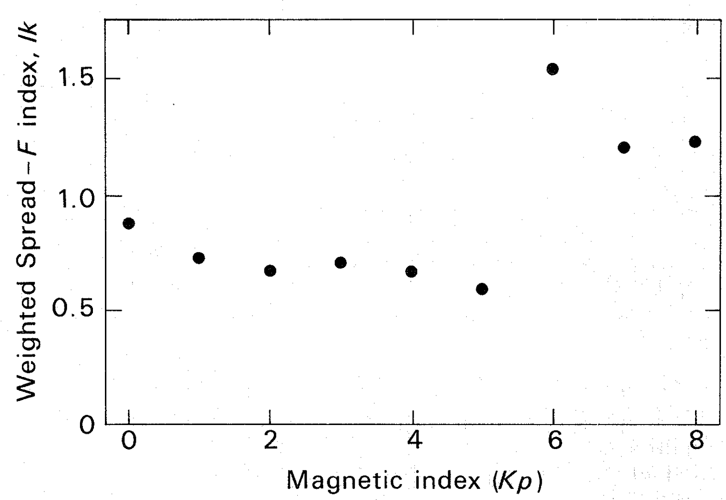

FIGURE 15

The variation in the occurrence of Spread-*F* at Argentine Islands with geomagnetic activity at sunspot maximum, for winter months (May–August). All data for $Kp \geq 8$ have been amalgamated and plotted at $Kp = 8$.

unexpected findings, which are contrary to observations made at other stations at similar magnetic latitudes, are discussed in more detail later. Insufficient Spread-*F* is observed during summer months at sunspot maximum to allow its variation in occurrence with magnetic activity to be established.

d. *Variation with geomagnetic activity between 1700 and 1900 LT.* The sunset period 1700–1900 LT was examined on the July data for both sunspot maximum and minimum using the technique described in section 5a. The *Ik* index for this 2-h period was compared with the index obtained from whole days' data. Fig. 16 shows that at both epochs of solar activity, the variations in the occurrence of Spread-*F* with geomagnetic activity at sunset was the same as during the rest of the day, to within experimental uncertainty.

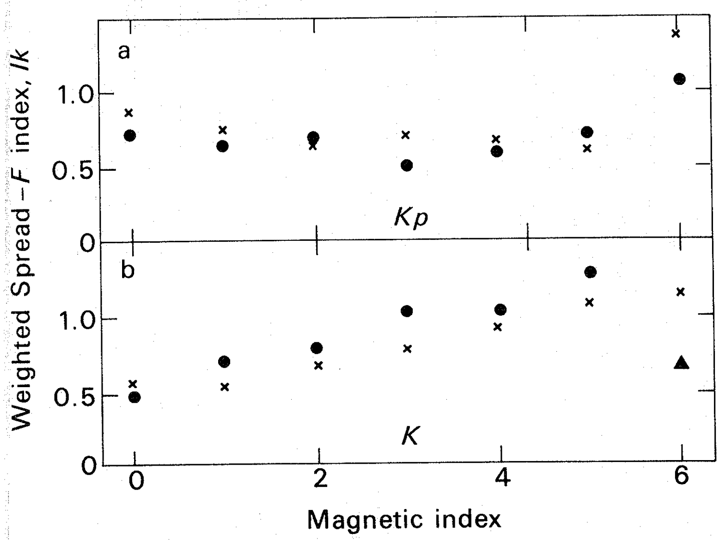

FIGURE 16
The variation in the occurrence of Spread-*F* at Argentine Islands in the period 1700–1900 LT with geomagnetic activity, (a) at sunspot maximum, and (b) at sunspot minimum. All data for $K \geq 6$ have been amalgamated and plotted at $K = 6$. ● *Ik* for period 1700–1900 LT (▲ point based on total of less than 24 hours' data); × *Ik* for entire day

6. *Dependence on ionospheric parameters*

a. *Maximum electron concentration.* The amount of Spread-*F* observed on ionograms may be dependent upon variations in the mechanism producing the irregularities, changes in the ambient electron concentration in the *F*-region or a combination of both factors. To assess what controls the amount of Spread-*F* on Argentine Islands ionograms, the hourly mean Spread-*F* has been plotted against the corresponding value of *foF2* for a summer and winter month at sunspot minimum (Fig. 17a) and for a winter month only at sunspot maximum (Fig. 17b). A horizontal line on these plots would suggest either that changes in electron concentration have no effect on the amount of Spread-*F* observed or that time variations of Spread-*F* production counteract exactly those resulting from changes in maximum electron concentrations; the latter appears very unlikely. Similarly a vertical line can be interpreted as the production mechanism totally dominating the time variations of Spread-*F*.

The winter data for sunspot minimum (Fig. 17a) may usefully be considered in two periods of local time (i) 2000–0700 LT (local night); (ii) 0700–2000 LT (local day). During the

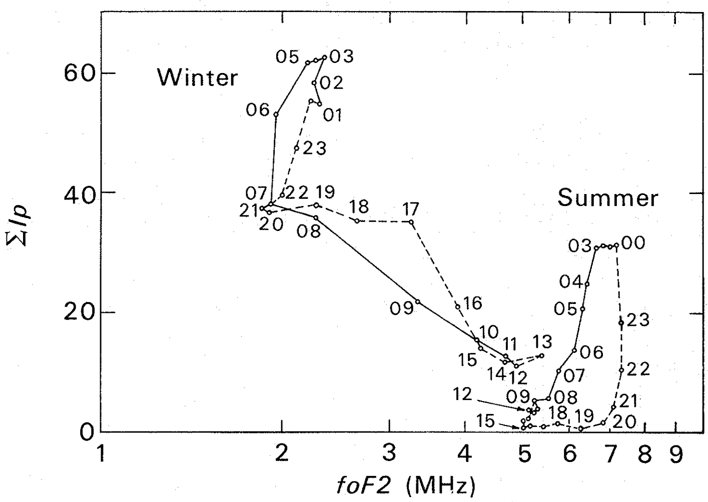

FIGURE 17a
The hourly mean Spread-*F* (ΣIp) plotted against the corresponding median values of *foF2*, for summer (November–February) and winter (May–August) at sunspot minimum, in order to demonstrate diurnal variation. The points are labelled with the local time in hours.

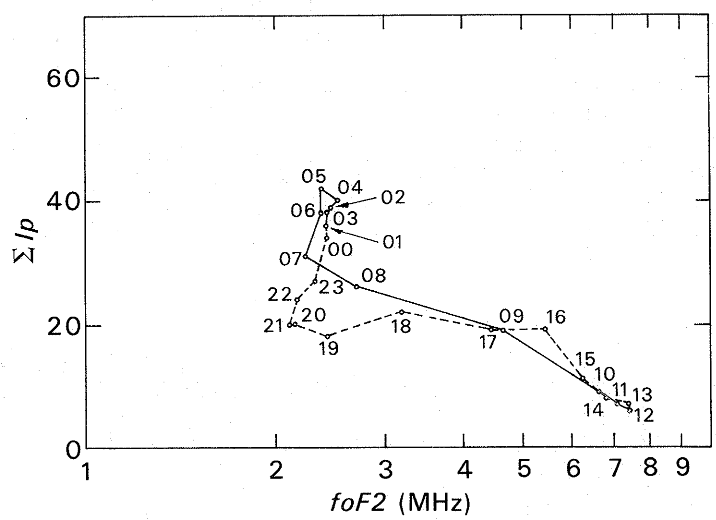

FIGURE 17b
The hourly mean Spread-*F* (ΣIp) plotted against the corresponding median value of *foF2*, for winter (May–August) at sunspot maximum. The points are labelled with the local time in hours.

local night, there is a large variation in the amount of Spread-*F* observed with little change in *foF2*. It can be concluded that there is a large variation in the effect producing irregularities with a maximum mean at 0300–0400 LT. During local day, Spread-*F* decreases fairly steadily as *foF2* increases. The lines of best fit (not shown) through the two parts of the data set (i and ii) are almost at right angles to each other. Hence, 0700 and 2000 can be regarded as key times when there is a change-over between regimes (i) and (ii).

The period 2000–0700 LT in the summer data (Fig. 17a) shows essentially the same pattern as in winter, the amount of Spread-*F* observed being almost completely dominated by variations in the production of irregularities, with the maximum occurring earlier, at 0000–0300 LT. From 0700 to 2000 LT there is very little Spread-*F* observed and so no firm conclusions can be drawn.

The winter sunspot maximum data (Fig. 17b) show a pattern very similar at all times to the corresponding sunspot minimum data, though the maximum effect of the irregularity production mechanism occurs about one hour later, near 0500 LT.

b. *hmF2 and ymF2.* To test whether the occurrence of Spread-*F* was dependent upon the height of the maximum electron concentration of the *F2*-layer, *hmF2* or the semi-thickness of the *F2*-layer, *ymF2,* values of these parameters were determined using a method proposed by Dudeney (1974). Table IV summarizes the correlations found but care should be used in interpreting these results as both *hmF2* and *ymF2* show diurnal, seasonal and solar cycle variations independent of Spread-*F* occurrence (see, for example, Dudeney, 1973).

TABLE IV

THE DIURNAL, SEASONAL AND SOLAR CYCLE CORRELATIONS OF *hmF2* AND *ymF2* WITH THE OCCURRENCE OF SPREAD-*F*

Parameter	*Diurnal*	*Seasonal*	*Solar cycle*
hmF2	Positive	None	Negative
ymF2	Positive	Negative	Negative

7. *Observations using the Doppler technique*

a. *Experimental methods.* An experiment using the Doppler principle was carried out on the Antarctic Peninsula from 1976 to 1979. The equipment consisted of three, stable, fixed-frequency transmitters located at Adelaide Island (lat. 67.8° S, long. 68.9° W), Almirante Brown (lat. 64.9° S, long. 62.9° W) and Palmer Station (lat. 64.8° S, long. 64.1° W) with a central receiving station at Argentine Islands (lat. 65.2° S, long. 64.3° W). The transmitting stations formed a triangle about the receiver. The operating frequency was selected in such a way as to ensure that the principal wave detected at the receiving station had only been reflected once from the *F*-region. The time intervals between recognizable features moving across the network can be used to determine their apparent horizontal velocities. In practice, two different frequencies were transmitted from each station allowing the vertical component of velocity to be resolved. (A more detailed explanation of the experiment and some preliminary observations are given by Dudeney and others (1977) and Dudeney and Jones (1976).)

A typical event showing the onset and development of Spread-*F* is illustrated in Fig. 18. The received signals from all stations show very little broadening of the frequency spectrum until about 0245 UT (2245 LT). The spectrum gradually widens over the next 3 h to a maximum of 3 Hz at 0540 UT.

Whenever broadening on the Doppler records was observed, Spread-*F* was always present on the corresponding Argentine Islands ionograms. The converse was not true. This is to be expected, as the ionosonde measures the vertical electron distribution up to *hmF2*, whereas the frequencies at which the Doppler experiment operates are usually refracted from well below *hmF2*.

b. *Interpretation of results.* The amount of Doppler broadening of the two traces from a single station should be in the ratio of the transmitted frequencies, assuming that the vertical

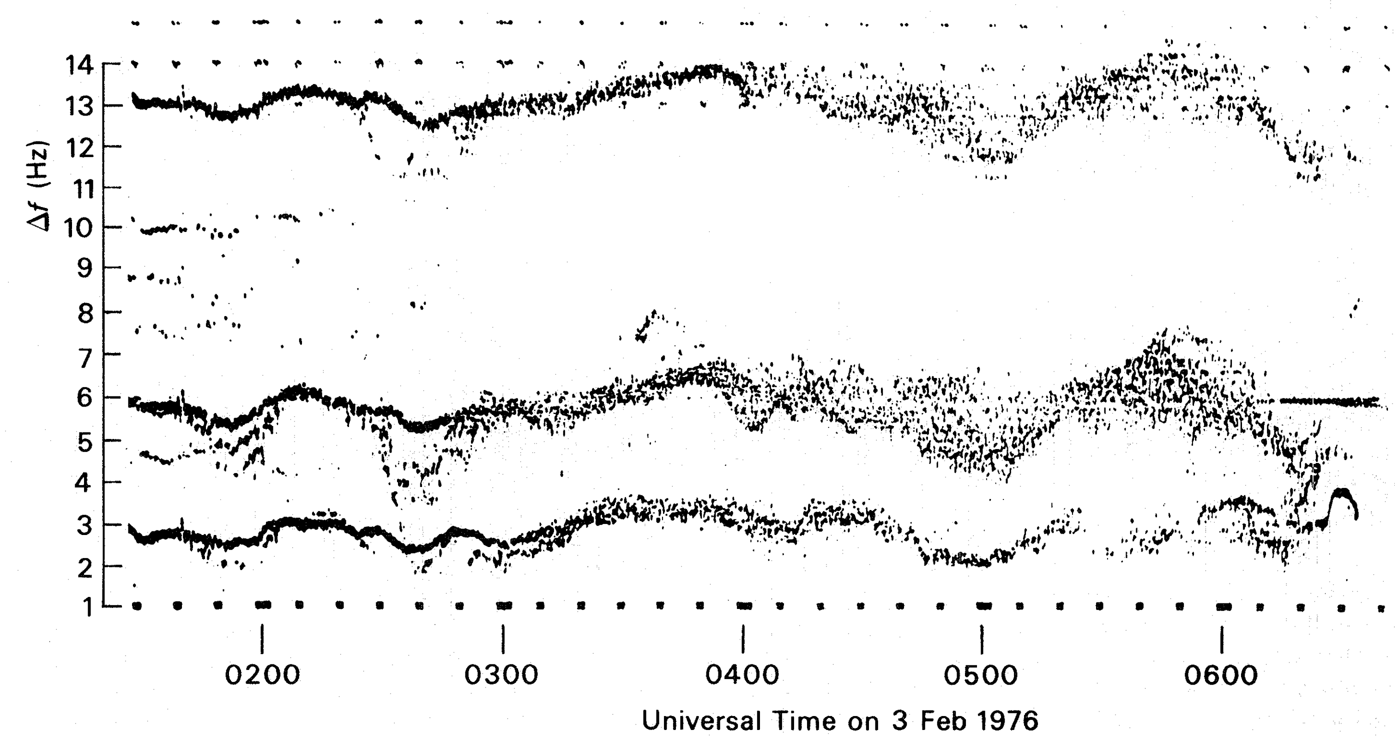

FIGURE 18

Doppler frequency changes measured at Argentine Islands on a signal frequency of 5.417 MHz for the period 0100–0600 UT on 3 February 1976, illustrating conditions when Spread-*F* occurs. The top trace is the signal transmitted from Almirante Brown, the middle trace from Palmer Station and the lower trace is from Adelaide Island.

electron concentration gradients near the reflection heights are the same, i.e. where dN/dh is the same for the two frequencies. However, on several occasions extensive broadening of the higher frequency signal has been observed on the Doppler data from Argentine Islands with little or no broadening on the lower frequency signal. No example of the converse has been observed.

One such case has been examined in detail for 18 March 1976. The ratio of the transmitted frequencies was 1.3 while the ratio of the frequency spread due to Doppler broadening was 2.5. The apogee heights of the two signals were determined to be 20 km apart and the difference in vertical electron concentration gradients at apogee was less than 10%. These values were determined using a sophisticated ray-tracing computer program (Jones and Stephenson, 1975). The electron density model used in these computations was that proposed by Dudeney (1978); this model gives good agreement between observed and theoretically predicted distributions at Argentine Islands.

It can be concluded that the variation in electron concentration gradient at the reflection points is insufficient to explain the observed differences in the Doppler data.

There are two possible interpretations of this observation. They are:

(a) that Spread-*F* irregularities are localized in height,

(b) that the system gain of the higher frequency signal is significantly greater than for the lower frequency spread.

The appearance of the final analogue output of the Doppler experiment depends upon a number of equipment parameters such as the gain of the receiver, aerials, recording and playback devices and losses along the ionospheric path of the signals. The differences in the latter for the case under consideration should be small as the take-off angles differ by less than 5°. Differences in the gains of the two independent systems also seem an unlikely explanation as on no occasion has more spreading been observed on the lower frequency channel despite periodic exchanges in parts of the equipment. More analysis of system gain is necessary but a tentative conclusion would be that (a) is more likely than (b) to explain the dissimilar amounts of broadening of the Doppler traces.

VII. THE STUDY OF SPREAD-*F* AT MAGNETICALLY CONJUGATE POINTS

1. *Correlation between Spread-F occurrence at geomagnetically conjugate points*

Argentine Islands (lat. 65° S, long. 64° W) and Wallops Island (lat. 38° N, long. 75° W) are well suited for conjugate studies, which are important when considering possible mechanisms for the production of Spread-*F* irregularities. Rodger (1976) showed that the correlation in the simultaneous occurrence of Spread-*F* at magnetically conjugate points was very significant, using data from Argentine Islands and Wallops Island. Fig. 19 gives additional examples from months including the two solstices and an equinox in 1973, which further support the results quoted. No correlation was found for the non-conjugate stations used for comparison, these being Ottawa, Port Stanley, Buenos Aires, Slough and Campbell Island. The significance of the correlations for three equinox and two solstice months in 1972–73 was established using a χ^2 test, the results of which are given in Table V. It is interesting to note that the χ^2 value decreases as the great circle distance between station and Argentine Islands (or its geomagnetic conjugate point) increases.

To determine whether the significance of the correlation varied seasonally, further data from the conjugate pair were analysed from the months January 1972 to September 1973. The months in this period were divided into three groups: equinox (March, April, September and October), Austral winter (May to August) and Austral summer (November to February). Values for χ^2 for these three groups, quoted in Table VI, show that the best correlation is at equinox but even during Austral summer there is a very high correlation in the simultaneous occurrence of Spread-*F*.

More detailed examination of this conjugate correlation shows that it is dominated by periods when (a) no Spread-*F* and (b) severe Spread-*F* is observed. Slightly spread conditions play little part in the correlation and, in effect, add noise to the data. The correlations were determined using an integrating period of a day, the 24-h period being chosen to run from 1200 LT on one day to 1159 LT on the next. The correlation of simultaneous occurrence is considerably reduced when

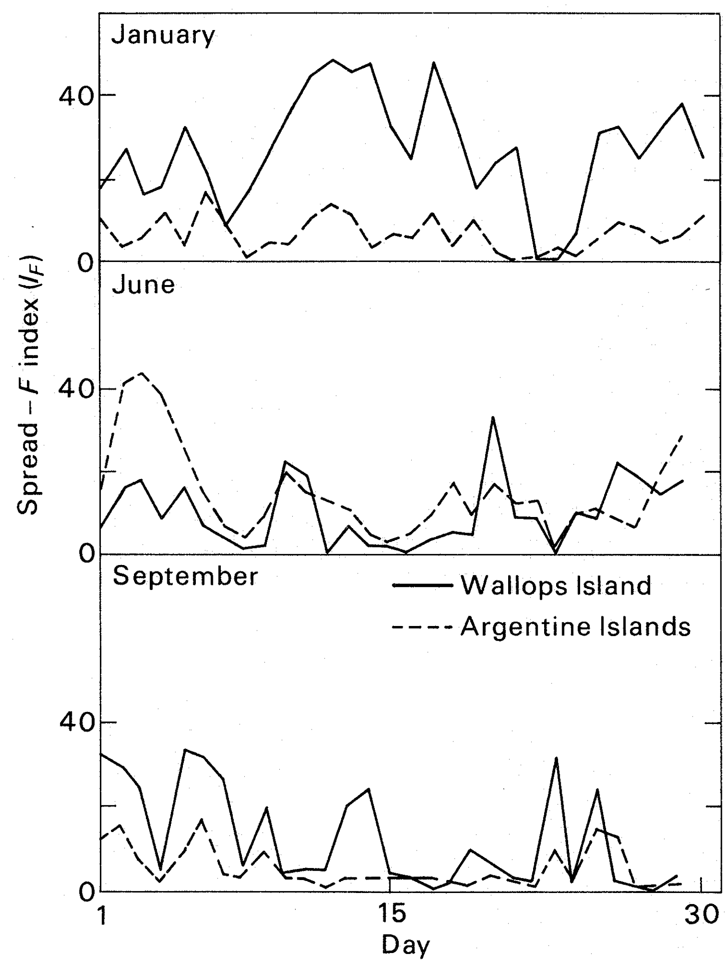

FIGURE 19

Variations in the occurrence of Spread-*F* at magnetically conjugate stations in 1973 during the course of an austral summer month (January), an austral winter month (June) and an equinox month (September). I_F is an index of the degree of Spread-*F* deduced from ionograms and published ionospheric data and is described fully in Rodger (1976).

TABLE V

CORRELATION BETWEEN SPREAD-*F* OCCURRENCE AT ARGENTINE ISLANDS (LAT. 65° S, LONG. 64° W) AND AT OTHER OBSERVATORIES

Observatory	*Latitude (degrees)*	*Longitude (degrees)*	χ^2 *value*	*Percentage probability that deviation greater than* χ^2 *would occur by chance*	*Great circle distances (km) from Argentine Islands or its conjugate magnetic point*
Wallops Island	38 N	75 W	26.2	$\leqslant$ 0.01	756
Ottawa	45 N	76 W	3.2	7.5	1209
Port Stanley	51 S	58 W	4.7	3.1	1548
Buenos Aires	34 S	58 W	1.6	21	3246
Slough	51 N	01 W	0.9	34	5336
Campbell Island	52 S	169 E	0.7	39	5626

TABLE VI

SEASONAL VARIATION IN THE CORRELATION OF THE SIMULTANEOUS OCCURRENCE OF SPREAD-*F* AT ARGENTINE ISLANDS AND WALLOPS ISLAND

Season	χ^2 *value*	*Percentage probability that deviation greater than* χ^2 *would occur by chance*
Equinox	33.2	$\leqslant$ 0.01
Austral winter	23.8	$\leqslant$ 0.01
Austral summer	13.7	0.06

the integrating period is reduced to an hour. Also, the duration of Spread-*F* on any one day was not directly related at the pair of observatories, but was controlled by the diurnal variation in occurrence of Spread-*F* at each location.

2. *Geomagnetic control of Spread-F*

Argentine Islands and Wallops Island have geographic latitudes differing by over 27° but they are approximately magnetically conjugate stations. Therefore, they are well placed for determining whether geographically or geomagnetically controlled mechanisms are primarily responsible for Spread-*F* production. Table VII shows the distribution of observed Spread-*F* among the seasons for the two observatories and the number of hours for which the solar zenith angle is less than 90° at a height of 250 km. There is no significant difference between the two observing stations in the percentage of Spread-*F* observed in a particular season, even at the solstices when differences in duration of sunlight are appreciable. It may be concluded that there is a strong geomagnetic control on the occurrence of Spread-*F*.

TABLE VII

RELATIVE AMOUNT OF SPREAD-*F* AT EACH SEASON FOR ARGENTINE ISLANDS AND WALLOPS ISLAND

	Percentage of all ionograms showing Spread-F echoes		*Hours of sunlight at a height of 250 km*	
Season	*Wallops Island*	*Argentine Islands*	*Wallops Island*	*Argentine Islands*
Summer	19	23	17.2	24.0
Equinox	25	24	14.2	17.0
Winter	56	53	11.8	9.9

3. *Geographic location and Spread-F*

It has already been shown that the diurnal variation in the occurrence of Spread-*F* at Argentine Islands is similar during summer and winter. This is clearly illustated in Fig. 20. The correlation coefficient of the line of best fit through these data is 0.7. The interesting point arising from this figure is the local hours which lie to the right of this line; these are 0500–0800 and 1600–2200 LT. For the majority of these hours the sun illuminates the ionosphere over the conjugate hemisphere but not the ionosphere over Argentine Islands in winter. This may be a further indication of the importance of the conjugate magnetic point in the production of Spread-*F* irregularities.

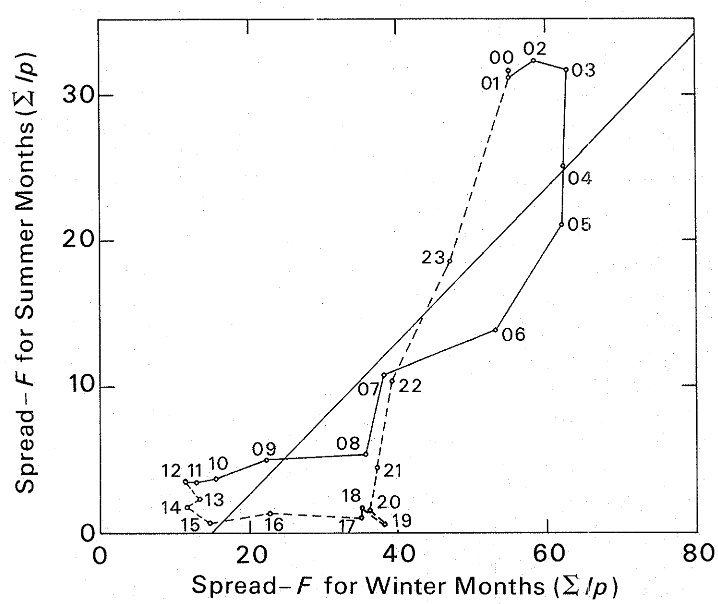

FIGURE 20

The mean hourly Spread-*F* occurrence above Argentine Islands during summer months (November–February) plotted against the corresponding mean for winter months (May–August) for a sunspot minimum period. The points are labelled with the local time in hours.

VIII. INTERPRETATION AND CONCLUSIONS

1. *Physical interpretation of ionogram classification*

Although Penndorf's (1962*a*) classification system for Spread-*F* observations was based only on pattern classification, some information about the distribution of irregularities and the shape of isoionic contours can be inferred from the patterns. Each of the patterns in Penndorf's scheme can be considered as a reflection from one or more of three spatial variations in electron concentrations. These three components are:

(a) an overhead structure giving a ray reflection,

(b) an oblique structure giving a ray reflection,

(c) irregularities giving rise to Spread-*F* reflections from either overhead or oblique structures.

For example, the ionogram in Fig. 1a results from horizontal isoionic contours with no irregularities, i.e. case (a). For Penndorf types $\alpha 1$ and $\alpha 2$, there is still a ray reflection from overhead, but reflections from irregularities are also observed, case (c). For types $\alpha 3$ to $\alpha 5$, which show considerable Spread-*F*, all recorded echoes are from irregularities which are sufficiently numerous to prevent there being a ray reflection. The variations in electron concentration within the irregularities is greatest for $\alpha 5$ and least for $\alpha 1$.

For the β, γ, ζ and η classes an argument can be proposed similar to that above, except that an oblique structure giving rise to ray reflection is also present. This implies that the isoionic contours above or near the station are not parallel to the ground.

The δ class of Spread-*F* (range Spread-*F*) was scaled when the ionogram traces broadened to more than twice normal width. This criterion can be fulfilled either by superposition of two or more ray structures, and or by smaller scale irregularity structures in the lower *F*-layer. In the classification system used, no differentiation was made between these types of δ class. The ϵ class of Spread-*F* arises only by diffuse reflections from irregularities.

2. *The size and orientation of irregularities*

Large disturbances with wavelengths greater than a Fresnel zone will give satellite traces or range Spread-*F* on ionograms. The Fresnel zone diameter, *d*, is given by $d \simeq 2\sqrt{\lambda h'}$ where λ is the free space wavelength of the sounding wave and h' is the virtual height of the layer. Experimental evidence (Bowman, 1960*a*, *b*) has shown that the isoionic contours for larger irregularities ($\lambda \gtrsim 20$ km) are not aligned with the magnetic field. Smaller irregularities ($\lambda \lesssim 20$ km) are normally field aligned (e.g. Bates, 1971). These smaller irregularities are responsible for producing frequency Spread-*F* on ionograms. One limitation is the determination of the smallest size of irregularity that the ionosonde can detect. Simple theory suggests that the minimum size for reflection in the plane perpendicular to the ray path of the wave should be half the sounding wavelength; however, the amplitude of these reflected signals could be below the threshold of the ionosonde.

The following observational points are also relevant:

(a) Spread-*F* signal amplitudes are about one order of magnitude less than those for ray reflections.

(b) The amount of Spread-*F* on the *o*- and *x*-traces is usually very similar both in extent and signal amplitude.

(c) The ratio of the echo amplitude of Spread-*F* echoes to the amplitude of a ray reflection is approximately the same for both the first order reflections and multiple echoes.

(d) If irregularities are present in the ionosphere, there is a considerable increase in the area of ionosphere which can reflect electromagnetic waves, compared with the undisturbed ionosphere.

3. *The diurnal, seasonal and solar cycle variations of Spread-F*

It has been shown that Spread-*F* is most likely to be observed at night, in winter during sunspot minimum. The probability of occurrence is least during the summer day at sunspot maximum. The winter diurnal variations of Spread-*F* show a sub-maximum in the early evening for which there is no corresponding peak in the summer data. The seasonal variations in occurrence do not show a sub-maximum in summer. These results are not consistent with the variations reported at other magnetic mid-latitude observatories.

Significantly more Spread-*F* (> 20%) is observed at all hours at sunspot minimum in winter compared with sunspot maximum, except 1600, 2000, 2100, 0600 and 0700 LT when approximately the same amount of Spread-*F* is observed. This result can be interpreted in terms of there being more than one mechanism responsible for the production of Spread-*F* irregularities.

The phenology of the Penndorf classes α, β and δ are summarized in Table VIII. α and β classes of Spread-*F* are very similar in their variations of occurrence but both differ markedly from the δ class. This indicates that the mechanism responsible for frequency Spread-*F* (α and β classes) is different from that for range Spread-*F* (δ class).

TABLE VIII

SUMMARY OF THE PHENOLOGY OF α, β AND δ CLASS SPREAD-*F*

	α	β	δ
Diurnal max. in occurrence (LT)	0300	0300–0400	0000
Seasonal max. in occurrence	Winter	Winter	Equinoxes
Correlation with solar activity	Negative	Negative	Negative

4. *Spread-F occurrence and geomagnetic activity*

There is a negative correlation between the occurrence of Spread-*F* and geomagnetic activity for $K \leqslant 5$ in winter at sunspot maximum. This is a new result. It differs from observations at Argentine Islands at sunspot minimum for both solstices and those reported from other middle latitude stations. Therefore these observations should provide an important test of any theory of Spread-*F* formation.

There is a significant increase in the occurrence of Spread-*F* for $Kp > 5$ at sunspot maximum in winter at Argentine Islands. This increase is associated with the poleward edge of the mid-latitude trough (Wrenn and Raitt, 1975) which shows considerably more Spread-*F* than either the trough minimum or the equatorial edge of the trough (Dudeney and Piggott, 1978). The mid-latitude trough has a characteristic signature on ionograms (Bellchambers and others, 1962; Piggott, 1975; Nygren, 1977); it is first observed at Argentine Islands at great obliquity when $Kp \simeq 4$ and is seen to move overhead when $Kp \geqslant 6$. This is consistent with the observation of the equator-ward movement of the mid-latitude trough during periods of increasing magnetic activity (Rycroft and Burnell, 1970; Rodger and Pinnock, 1980).

At sunspot minimum, the mean position of the mid-latitude trough is considerably poleward of its sunspot maximum position. At such times much larger magnetic storms are required to move this ionospheric feature over Argentine Islands during an epoch when very large storms are uncommon.

This result would suggest that either a different mechanism is responsible for Spread-*F* on the poleward edge of the mid-latitude trough, or the mechanisms involved in the production and maintenance of irregularities are significantly larger than those on the equatorial side of the trough. Particle precipitation is responsible for the formation of the poleward-edge enhancement of electron concentration (Pike and others, 1977) and may also have important effects on the production of irregularities.

5. *Spread-F and other ionospheric parameters*

Between 2000 and 0700 LT, the variations in the occurrence of Spread-*F* and *foF2* are very similar for the periods analysed (summer and winter at sunspot minimum and sunspot maximum winter) with only slight shifts in the local time at which maximum Spread-*F* is observed. Also between 0700 and 2000 LT, the two winter data sets from the different epochs of solar activity show great similarity. This is in complete contrast to the variations in the occurrence of Spread-*F* with geomagnetic activity which show a different phenology at sunspot maximum compared with sunspot minimum conditions.

6. *The H.F. Doppler experiment*

The most important observation made by the H.F. Doppler experiment, is the gradual increase in the amount of frequency spreading on the records over a period of 2–3 h (Fig. 18). This observation may be interpreted as a continuing excess in the number of irregularities being produced over those being destroyed. Another possible interpretation of the observations is that the original irregularity over Argentine Islands cascades, producing an increased number of smaller-sized irregularities in a manner similar to the process at equatorial and high latitudes. This cascading continues till either saturation is achieved, or the scale size of the irregularities being produced is below the resolution of the experiment. This mechanism is analogous to the breaking wave theory of Röttger (1976). However, the Doppler experiment data do not show the necessary amplification of waves prior to the onset of Spread-*F* for this theory to hold, but these waves may have wavelengths that are too small to be detected by the experimental configuration used.

It should be expected that there is a lower height limit for irregularities, and the Doppler experiment provides possible evidence for this. It is surprising that occasionally this limit is at *F*-region heights.

7. *Conjugate Spread-F observations*

The importance of the simultaneous occurrence of Spread-*F* at magnetically conjugate points has been emphasized. Also, significantly more Spread-*F* than would be expected is observed at Argentine Islands when the conjugate point is illuminated by the sun but Argentine Islands' ionosphere is not. These observations have significant bearing on any proposed mechanism for Spread-*F* irregularities.

Conjugacy effects have been noted before with phenomena such as geomagnetic pulsations, whistlers, aurorae, stable red arcs and the mid-latitude electron density trough. In all these examples, particle precipitation is of major importance, and may therefore also be important in the formation of Spread-*F* irregularities.

8. *Mechanisms of Spread-F production*

a. *Phenology of mechanisms.* Any mechanism for the production of Spread-*F* irregularities must be consistent with the observational evidence. The important observational points are summarized in Table IX.

TABLE IX

MAJOR RESULTS FROM ANALYSIS OF SPREAD-*F* AT ARGENTINE ISLANDS

Consistent with other observations at magnetic mid-latitudes	
Diurnal variation	Max. 0300–0400 LT; min. 1200–1400 LT
Seasonal variation	Max. in winter; min. in summer
Solar cycle variation	Negative correlation with solar activity
Geomagnetic activity	Positive correlation at sunspot minimum
New results	
Diurnal variation	Significant submaxima near 1700 and 0700 LT in winter only
Geomagnetic activity	Negative correlation at sunspot maximum for $Kp < 5$, with significant increase for $Kp \geqslant 6$
Conjugate Spread-*F*	Very significant positive correlation in occurrence with conjugate point in all seasons
Range Spread-*F*	Shows diurnal and seasonal variations in occurrence different from that of frequency Spread-*F*

It is apparent that the phenology of Spread-*F* is highly complex. Therefore, it would appear very unlikely that a single mechanism is responsible for the observed variations in the occurrence of Spread-*F*. It is suggested that there are at least four mechanisms each of which can be identified by a subset of observed phenology as follows:

Type 1 A mechanism showing strong diurnal variation, with a maximum in the early hours of the morning and a minimum near mid-day. The seasonal variation results in a maximum in winter. This mechanism must have the same diurnal pattern at both extremes of the solar cycle but its response to variations in magnetic activity must be fundamentally different at the two epochs.

Type 2 A mechanism which is only associated with the condition that the conjugate ionosphere is illuminated but Argentine Islands' ionosphere is in darkness. This type should show little or no solar cycle variation. It is required to explain the sub-maximum in occurrence of Spread-*F* in the early evening in austral winter.

Type 3 A mechanism for producing significant enhancements in the occurrence of Spread-*F* when the station lies poleward of the mid-latitude electron density trough.

Type 4 A mechanism to produce range Spread-*F* (δ class) which has a maximum diurnal occurrence at local midnight and a seasonal maximum at equinox.

The phenology of the *Type 1* mechanism is still relatively complex and could be the result of two mechanisms both of which have the same diurnal variations in occurrence but with one mechanism showing a positive correlation with magnetic activity and dominating at sunspot minimum; the other showing a negative correlation with magnetic activity and being more important at sunspot maximum.

b. *Height of irregularities.* The irregularities *Type 1* to *3* are observed near the height of maximum electron concentration of the *F*-layer, whilst *Type 4* are seen near the minimum height of the *F*-layer. However, none of these types need be restricted to the height range in which they are observed and could extend throughout the *F*-layer.

c. *Changes in recombination rate.* There are two important observations which show that localized changes in the recombination rate (either increases or decreases) cannot be responsible for the formation of Spread-*F* irregularities over Argentine Islands. First, Spread-*F* is often seen to form without any change in the maximum plasma frequency of the *F*-layer, *foF2*. Second, it is most unusual for Spread-*F* to be observed on the low frequency side of the main trace on ionograms (except during ionospheric modification experiments). These observations are incompatible with any model that relies on changes in recombination rate.

d. *Variations in production rate.* There are two major causes of the ionization in the ionosphere: solar electromagnetic radiation in the range of wavelengths 0.8–125 nm and particle precipitation (Rishbeth and Garriott, 1969).

As Spread-*F* is mainly a night-time phenomenon, solar radiation would appear to be a most unlikely source of irregularity production. At night, there is some scattering of Lyman α and β by the earth's geocorona (Tohmatsu and Wakai, 1970) but these lines are most efficient at ionizing molecular oxygen (Swider, 1965) which, although a major constituent below a height of 130 km at night, is only a very minor constituent in the *F*-region. Also, it is difficult to see how such a scattering mechanism could produce any of the observed diurnal, seasonal and solar cycle variations in the occurrence of Spread-*F*.

Particle precipitation has many attractive features as a source of irregularities in the *F*-region, as it can show great variability in both the time and space domains (Akasofu, 1968). Particles with folding energies of the order of a few hundred electron volts are mainly deposited at *F*-region heights (Rees, 1970). The distribution of these particles is not well established at geomagnetic mid-latitudes. However, Maehlum (1967), Manson and Merry (1970), Smith and others (1974), Voss and Smith (1980) and others have suggested that there may be a drizzle precipitation of low energy electrons which is not well correlated with geomagnetic activity.

The poleward edge of the mid-latitude trough is observed over Argentine Islands at sunspot maximum during very disturbed geomagnetic conditions ($Kp \geqslant 6$). Pike and others (1977) have suggested that the poleward edge of this feature is the result of soft particle precipitation and, therefore, is likely to be an important factor in the *Type 3* irregularity.

At high latitudes (L > 4) there are striking similarities in the occurrence of soft particle precipitation and Spread-*F*. For example, there is a maximum in precipitation of soft charged particles (50–1000 eV) at 73° geomagnetic on the night-side and about 83° geomagnetic on the day-side (Nelms and Chapman, 1970). This diurnal variation is approximately the same as that of the auroral oval when a maximum in the occurrence of Spread-*F* has been reported.

The importance of low energy particle precipitation in the production of Spread-*F* irregularities at Argentine Islands cannot be clearly established. There remains a need to analyse low energy particle precipitation data from satellites and corresponding ground-based ionosonde data for the occurrence of Spread-*F* at geomagnetic mid-latitudes.

e. *Transport of ionization.* There are several transport mechanisms which could be responsible for creating Spread-*F* irregularities, such as effects due to gravity waves and to electric fields. It is not yet possible to establish whether these are important at Argentine Islands but they cannot be rejected.

The data from the Argentine Islands La Cour magnetometer do not show any consistent feature before, during or after periods when Spread-*F* is observed. Although this may suggest that electric fields are not responsible for the formation of Spread-*F*, the *E*-region conductivity is very small under

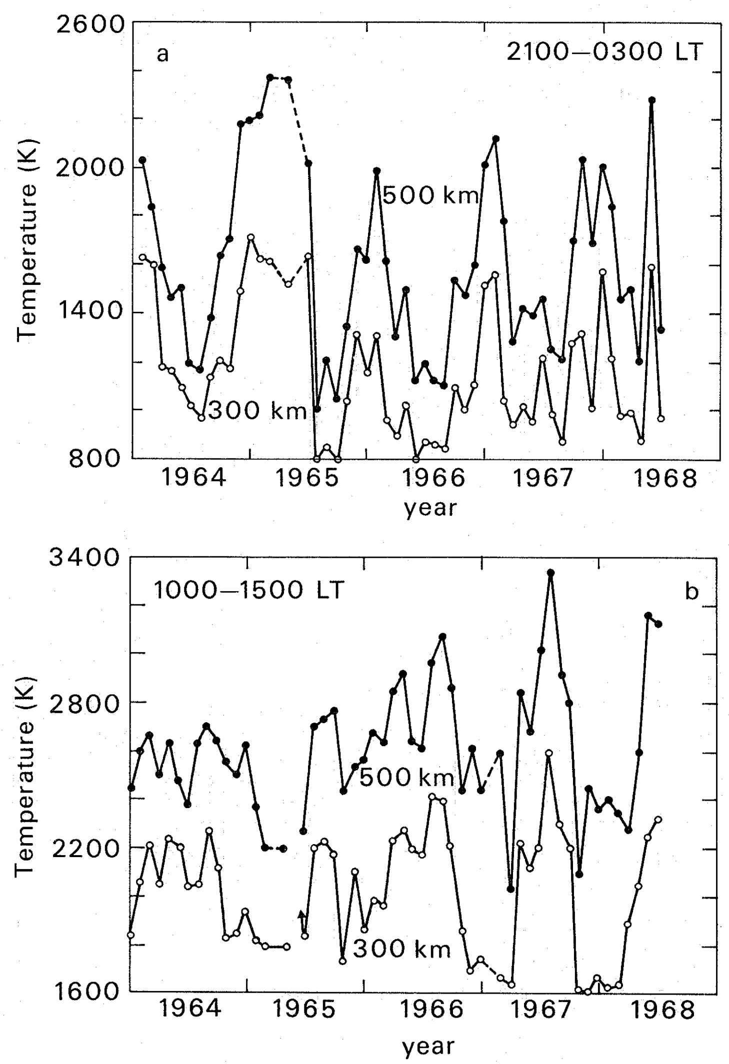

FIGURE 21
The seasonal variation in electron temperature determined at Millstone Hill over a 5-year period from 1964 to heights of 300 and 500 km (a) for night-time, and (b) for day-time. (After Evans, 1973.)

most conditions when Spread-*F* is seen (i.e. at night) and no definite conclusions can be made. Also a study of the occurrence of geomagnetic pulsations cannot be made at Argentine Islands as the sensitivity and time resolution of the magnetometer is too low. As several types of geomagnetic pulsation are associated with particle precipitation (e.g. Arthur and others, 1979) a morphological study of the phenomenon may help determine the importance of particle precipitation in the formation of Spread-*F* irregularities.

Plasma can be redistributed by gravity waves (Francis, 1975) and these have been suggested by Bowman (1960*a, c*), King (1970) and others as the most likely explanation for range Spread-*F* (*Type 4* irregularities) where the wavelength of the irregularity is greater than about 20 km. No evidence from the detailed studies at Argentine Islands has been found to contradict their conclusions. The effects on the distribution of plasma of shorter period waves with smaller wavelengths such as acoustic waves and infrasound have been completely neglected by those working on irregularities. These could be important in the formation of the irregularities responsible for frequency Spread-*F*.

The flow of photo-electrons with energies less than 70 eV from the illuminated ionosphere to the non-illuminated hemisphere is known to produce enhancement of 630-nm line radiation (Schaeffer, 1971) and increases in the electron temperature in the non-illuminated ionosphere (Doubin and others, 1968). These effects do not show systematic variations with time, which may result from small differences in electric potential between the ends of the magnetic field line. Little observational or theoretical work has been carried out on this inter-hemispheric electron flow. However, the enhancement in T_e may be important in the production of *Type 2* irregularities.

Plasma instability mechanisms are important in the formation of Spread-*F* irregularities in equatorial and high latitude regions (Fejer and Kelley, 1980). However, little detailed work has been carried out on this topic at geomagnetic mid-latitudes.

f. *Electron temperature and plasma concentration.* In the lower ionosphere (*D*- and *E*-regions), the collision frequencies between all neutral and ionic constituents are sufficiently high to maintain thermal equilibrium. Above about 130 km, this equilibrium cannot be established because the electron–ion and electron–neutral collision frequencies are too low. Thus, the mean temperature of the electron gas, T_e, can be substantially higher than that of the ions, T_i, and the neutrals, T_n (Rishbeth and Garriott, 1969). There are sufficient electron–electron collisions for the electron gas to achieve a Maxwell–Boltzmann temperature distribution, perhaps with a high energy tail of 'superthermal' electrons. The electron temperature is very variable with time (Rawer and others, 1978). There are a number of reasons for this such as variation

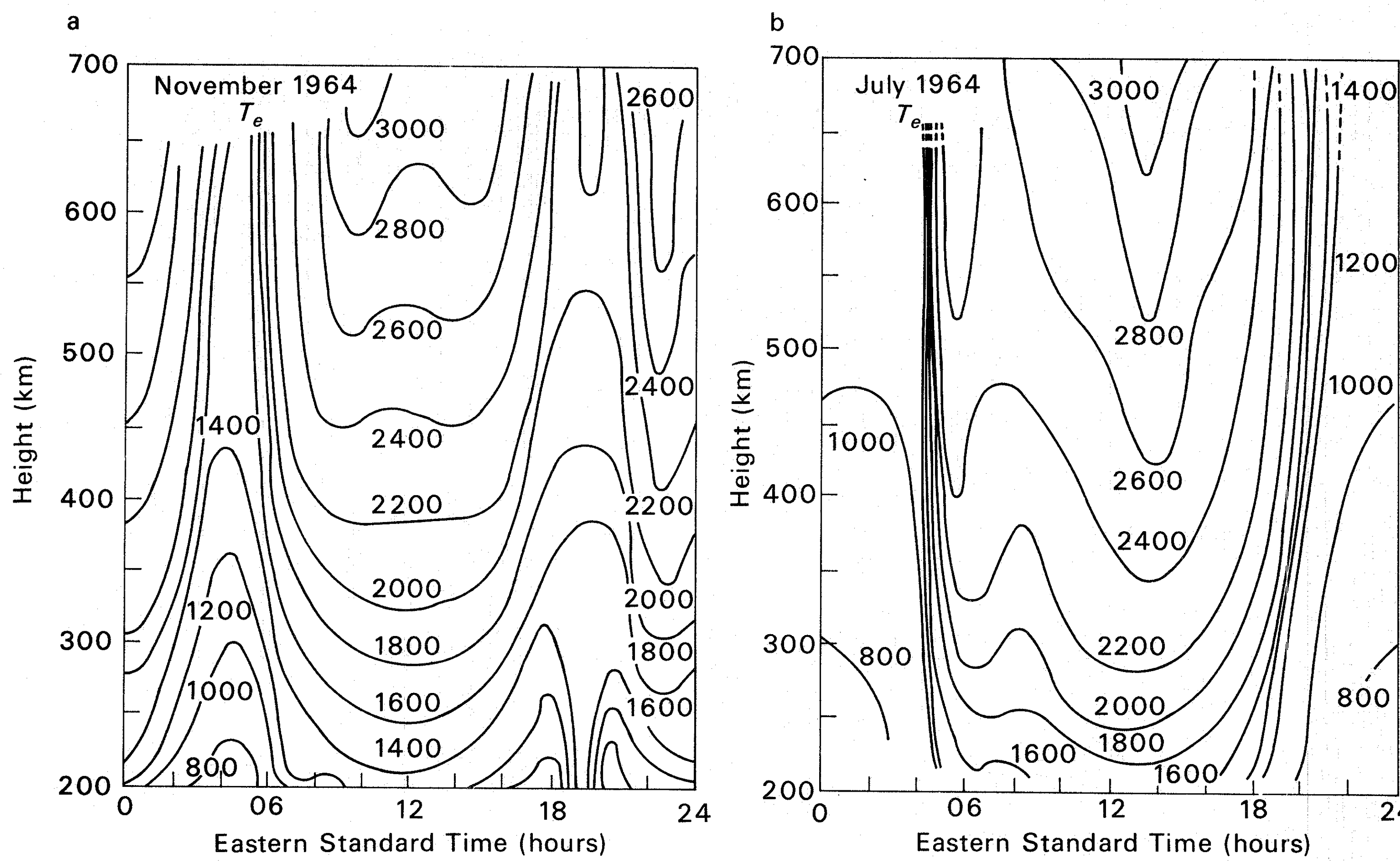

FIGURE 22
The diurnal variation in electron temperature with height at Millstone Hill at sunspot minimum (a) for winter, and (b) for summer. (After Evans, 1967.)

in the ion–electron collision frequency. Even at night, T_e can be substantially higher than T_i at *F*-region heights, which implies that there must be a heat source for the electrons. This could be, for example, soft particle precipitation or relatively hot thermal electrons from the protonosphere.

The solar cycle, seasonal and diurnal variations of T_e determined from the incoherent scatter radar data from Millstone Hill (lat. 43° N, long. 72° W) are shown in Figs. 21 and 22 and the most significant features have been summarized in Table X. The geomagnetic latitude of Millstone Hill is slightly higher than that of Argentine Islands, but its geographic latitude is significantly lower by 22°. The incoherent scatter radar data should be expected, in general, to show similar variations in T_e with time at the two locations. The largest difference in T_e should occur in austral summer when the sun illuminates the Argentine Islands ionosphere throughout the 24 h. T_e should then show little diurnal variation and its value should be relatively high. Whereas, at Millstone Hill, a significant diurnal variation in T_e is found (Fig. 22) at all seasons because the sun sets on the ionosphere every day.

TABLE X

SUMMARY OF ELECTRON TEMPERATURE RESULTS FROM MILLSTONE HILL

Winter	Two maxima in T_e, at 0000 and 1200 LT
	Two minima in T_e, at sunrise and sunset, with steep gradient in T_e at these times
Summer	Maximum in daytime, smaller maximum at night.
	Minimum at sunrise and sunset, with very steep gradient in T_e at these times
Solar cycle	Night time: No correlation
	Day time: Negative correlation in winter
	Positive correlation in summer

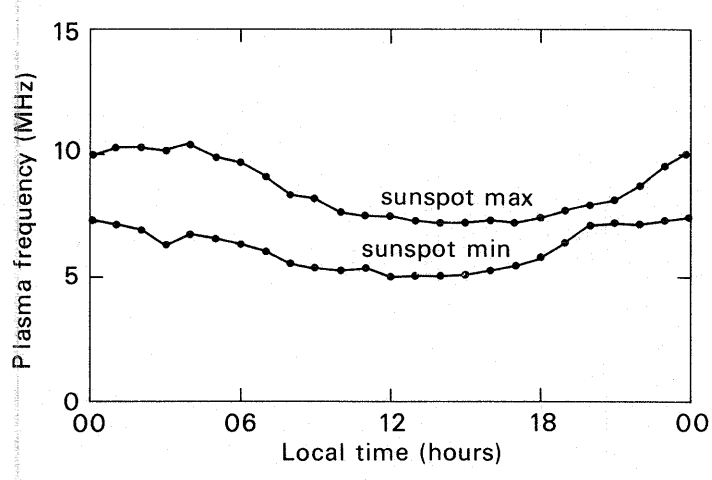

FIGURE 23

Mean diurnal variation in plasma frequency at Argentine Islands in summer for sunspot maximum and minimum.

Analysis of the effects of geomagnetic storms on the value of T_e, carried out by Evans (1970), again using Millstone Hill data, shows that T_e can be significantly enhanced (~ 100%) at night during sunspot minimum. However, changes in T_e do not directly relate to changes in *Kp*. There is little change in T_e during the day at sunspot minimum. Theoretical work (Chandra and Herman, 1969; Herman and Chandra, 1969)

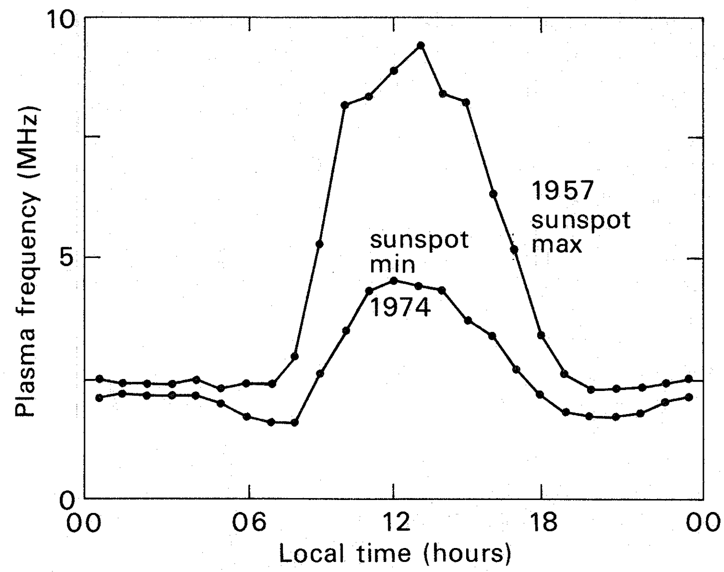

FIGURE 24

Mean diurnal variation in plasma frequency at Argentine Islands in winter for sunspot maximum and minimum.

suggests that at sunspot maximum there should be only minor enhancements of T_e during storms during both the day and the night.

The variations of T_e show some similarities to the variations of the *Type 1* irregularity. For example, both phenomena have a maximum at night, and night-time winter values exceed corresponding summer data. A high value of T_e cannot be the only condition necessary for Spread-*F* irregularity formation as T_e is also high when the ionosphere is directly illuminated by the sun. During these daytime periods, the maximum plasma frequency ($f_n \propto N_e^{1/2}$) is relatively high, as indicated in Figs. 23 and 24, which show the median summer and winter values for Argentine Islands at both sunspot maximum and

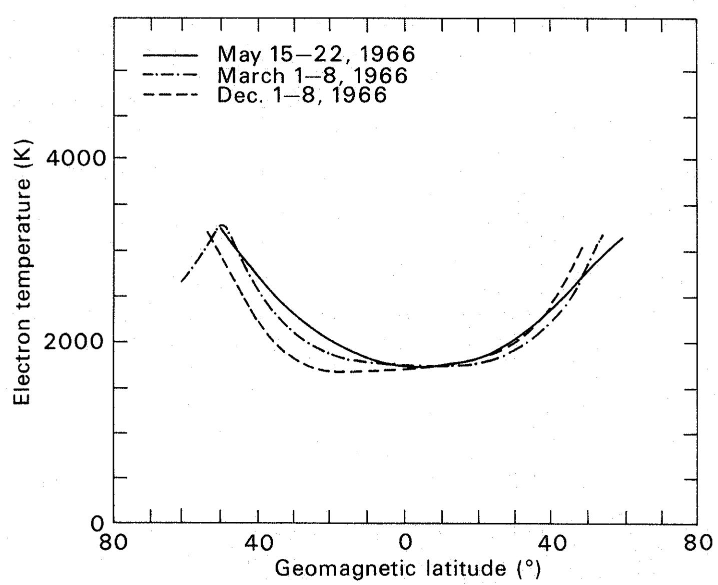

FIGURE 25

Latitudinal variation in electron temperature at a height of 2500 ± 500 km for three periods during 1966. (after Bauer, 1970.)

minimum. However, the ratio T_e/f_n shows great similarities to the observed variations in occurrence of the *Type 1* Spread-*F* irregularities throughout the day, season and solar cycle.

Further evidence of the similarities in the variations of electron temperature and Spread-*F* is provided by the series of latitude profiles of T_e for different seasons, shown in Fig. 25. These satellite measurements of T_e (from Bauer, 1970) were made at 2500 ± 500 km and show that T_e is relatively constant in equatorial regions but increases at middle latitudes in a very similar manner to the increases in the occurrence of Spread-*F* with latitude (Fig. 2).

Photoelectrons from the conjugate hemisphere increase the electron temperature in the non-illuminated ionosphere and these increases may be associated with *Type 2* irregularity mechanism.

Many workers (e.g. Wrenn and Raitt, 1975) show that electron temperature increases significantly in, and poleward of, the mid-latitude trough. This increase coincides with the region where significant enhancements in the occurrence of Spread-*F* are reported. Therefore, T_e may be an important parameter in the production of *Type 3* Spread-*F* irregularities.

The Debye length, λ, is another important parameter in plasma physics as it represents the distance beyond which the electrostatic field due to one particle is cancelled by the effects of a particle of opposite charge. The numerical expression for λ involves electron temperature and the reciprocal electron concentration. Thus the variation of Debye length shows many similarities to the variations of the occurrence of Spread-*F* at Argentine Islands. A more detailed examination of the variation of both T_e and N is needed to determine their importance in the formation and maintenance of Spread-*F* irregularities, and help to identify the plasma instability processes involved.

9. *Final remarks*

A detailed analysis of the occurrence of Spread-*F* over Argentine Islands, using mainly ionogram data, has shown that there are some similarities and several important differences in the occurrence of the phenomenon when a comparison is made with results from other observatories at geomagnetic middle latitudes. At least four types of irregularity are necessary to explain the observed complex phenology. Variations in electron temperature and the reciprocal of electron concentration with time show many similarities to the variations in the occurrence of Spread-*F*, suggesting that plasma instability mechanisms may be important in the production and maintenance of most of the irregularities over Argentine Islands. Also, particle precipitation and redistribution of ionization by gravity waves may be responsible for some of the irregularities observed.

IX. REFERENCES

Aarons, J., Mullen, J. P. *and* Whitney, H. E. 1969. The Scintillation Boundary. *Journal of Geophysical Research,* **74,** 884.

Allen, E. M., Thome, D. G., Rao, P. B. *and* St Germain, R. L. 1974. The angular distribution of Spread-*F* returns from an artificially modified ionosphere. *Journal of Geophysical Research,* **79,** 3161.

Akasofu, S. I. 1968. *Polar and magnetospheric substorms.* Dordrecht, D. Reidel Publishing Company.

Appleton, E. V. 1937. Regularities and irregularities in the ionosphere. *Proceedings of the Royal Society,* **162,** 451.

Arthur, C. W., Bjordal, J. *and* Rosenberg, T. J. 1979. *Pc* 3 magnetic pulsations and precipitation of energetic electrons. *Journal of Geophysical Research,* **84,** 4125.

Barrish, F. D. *and* Roederer, J. C. 1969. Conjugate intersects to selected geophysical stations. *International Council of Scientific Unions Solar–Terrestrial Physics Notes,* No. 4.

Bates, J. F. 1971. The aspect sensitivity of Spread-*F* irregularities. *Journal of Atmospheric and Terrestrial Physics,* **33,** 111.

Bauer, S. J. 1970. Temperature and composition studies in the polar ionosphere. (*In* Skovli, G., *ed. The polar ionosphere and magnetospheric processes.* New York, Gordon and Breach, 161–73.) (NATO Advanced Study Institute, Kjeller, Norway.)

Bellchambers, W. H., Barclay, L. W. *and* Piggott, W. R. 1962. Ionospheric observations. (*In* Brunt, D., *ed. The Royal Society IGY Expedition, Halley Bay, 1955–59.* Aberdeen, Aberdeen University Press.)

Booker, H. G. 1956. Theory of radar scattering from aurora. *Journal of Atmospheric and Terrestrial Physics,* **8,** 204.

Booker, H. G. *and* Wells, H. W. 1938. Scattering of radiowaves by the *F*-region of the ionosphere. *Terrestrial Magnetism and Atmospheric Electricity,* **43,** 249.

Bowman, G. G. 1960*a*. A relationship between Spread-*F* and the height of the ionospheric *F2*-layer. *Australian Journal of Physics,* **13,** 69.

Bowman, G. G. 1960*b*. Further studies of 'Spread-*F*' at Brisbane—I. Experimental. *Planetary and Space Science,* **2,** 133.

Bowman, G. G. 1960*c*. Further studies of 'Spread-*F*' at Brisbane—II. Interpretation. *Planetary and Space Science,* **2,** 150.

Bowman, G. G. 1971. What is the origin of Spread-*F*? *Nature,* **229,** 117.

Bowman, G. G. 1979. Latitude dependence of the time delay in Spread-*F* occurrence following geomagnetic activity. *Journal of Atmospheric and Terrestrial Physics,* **41,** 999.

Brace, L. H., Theis, R. G. *and* Dalgarno, A. 1973. The cylindrical electrostatic probes for Atmospheric Explorer-C, -D and -E. *Radio Science,* **8,** 341.

Briggs, B. H. 1958. The diurnal and seasonal variations of Spread-*F* ionospheric echoes and scintillation of a radio star. *Journal of Atmospheric and Terrestrial Physics,* **12,** 88.

Chandra, S. *and* Herman, J. R. 1969. *F*-region ionisation and heating during magnetic storms. *Planetary and Space Science,* **17,** 841.

Chandra, S. *and* Rastogi, R. G. 1972. Equatorial Spread-*F* over a solar cycle. *Annales de Geophysique,* **28,** 709.

Clarke, C. *and* Shearman, E. D. R. 1953. Automatic ionospheric height recorder. *Wireless World,* **30,** 211.

Clemensha, B. R. 1964. An investigation of the irregularities in the *F*-region associated with equatorial type Spread-*F*. *Journal of Atmospheric and Terrestrial Physics,* **26,** 91.

Doubin, M. L., Lejeune, G., Petit, M. *and* Weill, G. M. 1968. Excitation of the oxygen lines and ionospheric heating by conjugate photoelectrons. *Journal of Atmospheric and Terrestrial Physics,* **30,** 299.

Dudeney, J. R. 1973. *Studies based on the Antarctic ionospheric F-layer.* Ph.D. thesis, University of London. (Unpublished.)

Dudeney, J. R. 1974. A simple empirical model for estimating the height and semi-thickness of the *F2*-layer at Argentine Islands, Graham Land. *British Antarctic Survey Scientific Reports,* No. 88, 46 pp.

Dudeney, J. R. 1978. An improved model of the variation of electron concentration with height in the ionosphere. *Journal of Atmospheric and Terrestrial Physics,* **40,** 195.

Dudeney, J. R. *and* Jones, T. B. 1976. Doppler radio soundings of the ionosphere over the Antarctic Peninsula. *Antarctic Journal of the United States,* **11,** 102.

Dudeney, J. R. *and* Piggott, W. R. 1978. Antarctic Ionospheric Research. (*In* Lanzerotti, L. J. *and* Park, C. G., *eds. Upper atmospheric research in Antarctica.* Washington, American Geophysical Union, 200–35.)

DUDENEY, J. R., JONES, T. B., KRESSMAN, R. I. *and* SPRACKLEN, C. T. 1977. Radio-wave studies of the Antarctic ionosphere. *Philosophical Transactions of the Royal Society of London, Series B,* **279,** 239.

EVANS, J. V. 1967. Mid-latitude *F*-region densities and temperatures at sunspot minimum. *Planetary and Space Science,* **15,** 1387.

EVANS, J. V. 1969. Theory and practice of ionospheric study by Thomson scatter radar. *Proceedings of the Institute of Electrical and Electronic Engineers (USA),* **57,** 496.

EVANS, J. V. 1970. Mid-latitude ionospheric temperatures during three magnetic storms. *Journal of Geophysical Research,* **75,** 4803.

EVANS, J. V. 1973. Seasonal and sunspot cycle variations of *F*-region electron temperatures and photo-ionospheric heat fluxes. *Journal of Geophysical Research,* **78,** 2344.

EVANS, J. V. 1974. Some post-war developments in ground based radiowave sounding of the ionosphere. *Journal of Atmospheric and Terrestrial Physics,* **36,** 2183.

FARLEY, D. T. 1963. A plasma instability resulting in field-aligned irregularities in the ionosphere. *Journal of Geophysical Research,* **68,** 6083.

FARLEY, D. T. 1967. A theory of incoherent scattering of radio waves by a plasma. *Journal of Geophysical Research,* **72,** 91.

FARLEY, D. T., BALSLEY, B. B., WOODMAN, R. F. *and* MCCLURE, J. P. 1970. Equatorial Spread-*F*; implications of VLF radio observations. *Journal of Geophysical Research,* **75,** 7199.

FEJER, B. G. *and* KELLEY, M. C. 1980. Ionospheric irregularities. *Reviews of Geophysics and Space Physics,* **18,** 401.

FRIHAGEN, J. 1970. Irregularities in the electron density of the polar ionosphere. (*In* SKOVLI, G., *ed. The polar ionosphere and magnetospheric processes.* New York, Gordon and Breach, 271–84.) (NATO Advanced Study Institute, Kjeller, Norway.)

FRIHAGEN, J. 1971. Occurrence of high latitude ionospheric irregularities giving rise to satellite scintillations. *Journal of Atmospheric and Terrestrial Physics,* **33,** 21.

FRANCIS, S. H. 1975. Global propagation of atmospheric gravity waves—a review. *Journal of Atmospheric and Terrestrial Physics,* **37,** 1011.

GLEDHILL, J. A. *and* HOFFMAN, R. A. 1981. Night-time observations of 0.2–26 keV charged particles in the South Atlantic Anomaly made by Atmospheric Explorer-C. *Journal of Geophysical Research,* **82,** 6739.

HANSON, W. B., ZUCCARO, D. R., LIPPINCOTT, C. R. *and* SANATANI, S. 1973. The retarding-potential analyzer on Atmospheric Explorer. *Radio Science,* **8,** 333.

HEISLER, L. H. *and* WILSON, L. D. 1962. Spread-*F* development associated with a high altitude nuclear explosion. *Nature,* **196,** 258.

HERMAN, J. R. 1966. Spread-*F* and the ionospheric *F*-region. *Reviews of Geophysics and Space Physics,* **4,** 255.

HERMAN, J. R. *and* CHANDRA, S. 1969. The influences of varying solar flux on ionospheric temperatures and densities. *Planetary and Space Science,* **17,** 815.

HOLTET, J. A., MAYNARD, N. C. *and* HEPPNER, J. P. 1976. Variational electric fields and their relation to Spread-*F* and plasma irregularities. *Goddard Space Flight Centre Report* X-625-76-24.

INAG, 1969. *Ionospheric Network Advisory Group Bulletin,* No. 1, 9.

JONES, R. M. *and* STEPHENSON, J. J. 1975. A versatile three-dimensional ray tracing computer program for radio waves in the ionosphere. *US Department of Commerce, Office of Telecommunications Report* **75–76,** 197.

KASUYA, I., KATANO, S. *and* TAGUCHI, S. 1955. The occurrence of Spread-*F* echoes in the *F*-region over Japan. *Journal of the Radio Research Laboratories (Japan),* **2,** 259.

KELLEY, M. C. 1979. Equatorial Spread-*F*: a review of recent experimental results in wave instabilities in space plasma. (*In* PALMADESSO, P. J. *and* PAPADOPOULOS, K., *eds. Wave instabilities in space plasma.* Dordrecht, D. Reidel Publishing Company, 291–306).

KING, G. A. M. 1970. Spread-*F* on ionograms. *Journal of Atmospheric and Terrestrial Physics,* **32,** 209.

KING, J. W., LEGG, A. J. *and* SMITH, P. A. 1967. Observations of Spread-*F* ionisation in the topside of the ionosphere. *Journal of Atmospheric and Terrestrial Physics,* **29,** 1373.

KOSTER, J. R. 1958. Radio star scintillations at an equatorial station. *Journal of Atmospheric and Terrestrial Physics,* **12,** 100.

KOSTER, J. R. *and* WRIGHT, R. W. 1960. Scintillation Spread-*F* and trans-equatorial scatter. *Journal of Geophysical Research,* **65,** 2303.

MAEHLUM, B. 1967. On the winter anomaly in the mid-latitude *D*-region. *Journal of Geophysical Research,* **72,** 2287.

MANSON, A. H. *and* MERRY, M. W. J. 1970. Particle influx and the winter anomaly in the mid-latitude (L = 2.5–3.5) lower ionosphere. *Journal of Atmospheric and Terrestrial Physics,* **32,** 1169.

MAWDSLEY, J. *and* WARD, W. H. 1960. Field aligned ionisation. *Journal of Geophysical Research,* **65,** 1929.

MCILWAIN, C. E. 1961. Co-ordinates for mapping the distribution of magnetically trapped particles. *Journal of Geophysical Research,* **66,** 3681.

NELMS, G. L. *and* CHAPMAN, J. H. 1970. The high latitude ionosphere: results from the Alouette/ISIS topside sounders. (*In* SKOVLI, G., *ed. The polar ionosphere and magnetospheric processes.* New York, Gordon and Breach, 233–69.) (NATO Advanced Study Institute, Kjeller, Norway.)

NYGREN, T. 1977. Simulation of vertical incidence ionograms by ray tracing method in the presence of replacement layer and ionospheric trough. *Journal of Atmospheric and Terrestrial Physics,* **39,** 733.

OSSAKOW, S. L. 1979. A review of recent results on Spread-*F* theory. (*In* PALMADESSO, P. J. *and* PAPADOPOULOS, K. *eds. Wave instabilities in space plasmas,* Dordrecht, D. Reidel Publishing Company.)

PENNDORF, R. 1962*a*. Classification of Spread-*F* on ionograms. *Journal of Atmospheric and Terrestrial Physics,* **24,** 771.

PENNDORF, R. 1962*b*. Geographic distribution of Spread-*F* in Arctic. *Journal of Geophysical Research,* **67,** 2279.

PENNDORF, R. 1962*c*. Diurnal and seasonal variations of Spread-*F* in Arctic. *Journal of Geophysical Research,* **67,** 2289.

PERKINS, F. 1973. Spread-*F* and ionospheric currents. *Journal of Geophysical Research,* **78,** 218.

PETIT, M. 1975. Incoherent scatter radar results. (*In* MCCORMAC, B. M., *ed. Atmospheres of Earth and planets.* Dordrecht, D. Reidel Publishing Company, 159–74.)

PIGGOTT, W. R. 1975. *High latitude supplement to the URSI handbook of ionogram interpretation and reduction.* Washington, D.C., U.S. World Data Center A. (N.O.A.A. Report UAG-50.)

PIGGOTT, W. R. 1977. The importance of the Antarctic in Atmospheric Sciences. *Philosophical Transactions of the Royal Society of London, Series B,* **279,** 275.

PIGGOTT, W. R. *and* RAWER, K. 1972. *URSI handbook of ionogram interpretation and reduction,* 2nd Edition. Washington, D.C., US Department of Commerce. (N.O.A.A. Report UAG-23.)

PIGGOTT, W. R. *and* RAWER, K. 1978. *URSI handbook of ionogram interpretation and reduction,* 2nd Edition (revised). Washington D.C., World Data Center A (N.O.A.A. Report UAG-23A.)

PIKE, C. P., WHALEN, J. A. *and* BUCHAU, J. 1977. A 12-hour case study of auroral phenomena in the midnight sector: *F*-layer and 6 300 Å measurements. *Journal of Geophysical Research,* **82,** 3547.

RAO, M. S. V. G., RAO, B. R., RAO, P. R. A. *and* PANT, R. 1960. Correlation of Spread-*F* activity with *F*-region height changes. *Journal of Atmospheric and Terrestrial Physics,* **17,** 345.

RAWER, K., BILITZA, D. *and* RAMARKRISHNAN, S. 1978. Goals and status of the international reference ionosphere. *Reviews of Geophysics and Space Physics,* **16,** 117.

RATCLIFFE, J. A. 1959. *The magneto-ionic theory and its application to the ionosphere.* Cambridge, Cambridge University Press.

REES, M. H. 1970. The effects of low energy precipitation on the upper atmosphere. (*In* SKOVLI, G., *ed. The polar ionosphere and magnetospheric processes.* New York, Gordon and Breach, 137–49.) (NATO Advanced Study Institute, Kjeller, Norway.)

RENAU, J. 1959. A theory of Spread-*F* based on a scattering screen model. *Journal of Geophysical Research,* **64,** 971.

RENAU, J. 1960. A study of observed Spread-*F*. *Journal of Geophysical Research,* **65,** 3219.

RISHBETH, H. *and* GARRIOTT, O. K. 1969. *Introduction to ionospheric physics.* London, Academic Press.

RODGER, A. S. 1976. The simultaneous occurrence of Spread-*F* at magnetically conjugate points. *Journal of Atmospheric and Terrestrial Physics,* **38,** 1365.

RODGER, A. S. *and* PINNOCK, M. 1980. The variability and predictability of the main ionospheric trough. (*In* DEEHR, C. S. *and* HOLTET, J. A., *eds. Exploration of the polar upper atmosphere.* Dordrecht, D. Reidel Publishing Company, 463–9.) (NATO Advanced Study Institute, Lillehammer, Norway.)

RODGER, A. S., BOTELER, D. H. *and* DUDENEY, J. R. 1981. The importance of the maximum plasma frequency of the ionosphere in controlling the occurrence of blackout. *Journal of Atmospheric and Terrestrial Physics,* **43,** 1243–9.

RÖTTGER, J. 1976. The macrostructure of equatorial Spread-*F* irregularities. *Journal of Atmospheric and Terrestrial Physics,* **38,** 97.

RYCROFT, M. J. *and* BURNELL, S. J. 1970. Statistical analysis of movements of the ionospheric trough and the plasmapause. *Journal of Geophysical Research,* **75,** 5600.

SASTRI, J. H., MURTHY, B. S. *and* SASIDHARAN, K. 1975. On the characteristics of Spread-*F* configurations at Kodaikanal. *Annales de Geophysique,* **31,** 409.

SCANNEPIECO, A. J., GOLDMAN, S. R., OSSAKOW, S. L., BROOK, D. L. *and* McDONALD, B. E. 1975. *Theoretical and numerical simulation studies of mid-latitude F-region irregularities.* Washington D.C., Naval Research Laboratory. (NRL Memorandum Report 3014.)

SCHAEFFER, R. 1971. The role of recombination in the pre-dawn enhancement of λ 6300 Å [OI] airglow. *Journal of Atmospheric and Terrestrial Physics,* **33,** 437.

SHIMAZAKI, T. 1959. A statistical study of world-wide occurrence probability of Spread-*F*. Part I. Average state. Part II. Abnormal state in severe magnetic storms. *Journal of the Radio Research Laboratories (Japan),* **6,** 669.

SHIMAZAKI, T. 1960. The occurrence of Spread-*F* and the geomagnetic field. *Journal of the Radio Research Laboratories (Japan),* **7,** 437.

SINGLETON, D. G. 1957. A study of Spread-*F* ionospheric echoes at night at Brisbane, III. Frequency spreading. *Australian Journal of Physics,* **19,** 60.

SINGLETON, D. G. 1960. The geomorphology of Spread-*F*. *Journal of Geophysical Research,* **65,** 3615.

SINGLETON, D. G. 1968. The morphology of Spread-*F* occurrence over half a sunspot cycle. *Journal of Geophysical Research,* **73,** 295.

SINGLETON, D. G. 1969. The occurrence of scintillations in 1972 producing irregularities over Australia. *Journal of Geophysical Research,* **74,** 1772.

SKINNER, N. J. *and* KELLEHER, R. F. 1971. Studies of *F*-region irregularities at Nairobi: I. From Spread-*F* on ionograms, 1964–1970. *Annales de Geophysique,* **27,** 181.

SMITH, L. G., GELLER, M. A. *and* VOSS, M. D. 1974. Energetic electrons in the mid-latitude night-time *E*-region. *Journal of Atmospheric and Terrestrial Physics,* **36,** 1601.

SWIDER, W. 1965. A study of the night-time ionosphere and its reaction rates. *Journal of Geophysical Research,* **70,** 4859.

TITHERIDGE, J. E. 1971. The diffraction of satellite signals by isolated ionospheric irregularities. *Journal of Atmospheric and Terrestrial Physics,* **33,** 47.

TOHMATSU, T. *and* WAKAI, N. 1970. An investigation of night-time ionizing sources in the low and mid-latitudes. *Annales de Geophysique,* **26,** 209.

TURUNEN, T. *and* OKSMAN, J. 1979. On the relative location of the plasmapause and the H.F. backscatter curtains. *Journal of Atmospheric and Terrestrial Physics,* **41,** 345.

UTLAUT, W. F. 1970. Radio wave modification of the ionosphere; some ionosonde observations of ionosphere modification experiment at very high power, high frequency, ground-based transmission. *Journal of Geophysical Research,* **75,** 6429.

VOSS, H. D. *and* SMITH, L. G. 1980. Global zones of energetic particle precipitation. *Journal of Atmospheric and Terrestrial Physics,* **42,** 227.

WOODMAN, R. F. 1970. Vertical drift velocities and east–west electric fields at the magnetic equator. *Journal of Geophysical Research,* **75,** 6249.

WRENN, G. *and* RAITT, W. J. 1975. *In situ* observations of mid-latitude ionospheric phenomena associated with the plasmapause. *Annales de Geophysique,* **31,** 17.